

**Preparation and Characterization of Co-Fe/Al<sub>2</sub>O<sub>3</sub> Catalyst for Steam  
Reforming of Ethanol**

by

Nursyazwani Bt Zainal Abidin

9530

Dissertation submitted in partial fulfilment of  
the requirements for the  
Bachelor of Engineering (Hons)  
(Chemical Engineering)

JULY 2010

Universiti Teknologi PETRONAS

Bandar Seri Iskandar

31750 Tronoh

Perak Darul Ridzuan

**CERTIFICATION OF APPROVAL**

**PREPARATION AND CHARACTERIZATION OF Co-Fe/Al<sub>2</sub>O<sub>3</sub>  
CATALYST FOR STEAM REFORMING OF ETHANOL**

by

Nursyazwani Binti Zainal Abidin

A project dissertation submitted to the

Chemical Engineering Programme

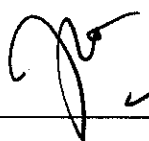
Universiti Teknologi PETRONAS

in partial fulfillment of the requirement for the

BACHELOR OF ENGINEERING (HONS)

(CHEMICAL ENGINEERING)

Approved by,

  
DR ANITA RAMLI  
Associate Professor  
Fundamental & Applied Sciences Department  
Universiti Teknologi PETRONAS, PERAK

(AP. DR. Anita Bt. Ramli)

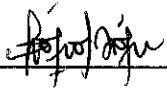
UNIVERSITI TEKNOLOGI PETRONAS

TRONOH, PERAK

JULY 2010

## CERTIFICATION OF ORIGINALITY

This is to certify that I am responsible for the work submitted in this project, that the original work is my own except as specified in the references and acknowledgements, and that the original work contained herein have not been undertaken or done by unspecified sources or persons.



---

(NURSYAZWANI BINTI ZAINAL ABIDIN)

## ABSTRACT

Steam reforming of ethanol has been studied using various catalysts. Bi-metallic catalysts which are Cobalt and Iron supported on Aluminium Oxide is one of the candidates for steam reforming of ethanol that is capable to produce hydrogen. Iron loading on Cobalt had a positive effect on promotion of the catalytic activity of steam reforming of ethanol. The combination of Cobalt and Iron gives high stability, longer lifetime and resulted as active metal. The catalyst was prepared using incipient wetness method, with sequential impregnation, co-impregnation and different molar ratio. The precursor was impregnated for 6 hours, dried for 16 hours, calcined at 500°C for 16 hours and have characterized using XRD, SEM and BET. The XRD pattern obtained was compared to analyze the crystalline phase observed in the samples. Result of high intensity of the peak is due to the overlapping of metal with the support catalyst. The SEM micrographs indicate that the alumina is crystalline with a well- defined plane exposed and that both metals coated on the support surface uniformly. From BET, the catalyst surface area and dispersion are shown as functions of metal loading for the various series of impregnation and ratio.

## ACKNOWLEDGEMENT

Alhamdulillah, first and foremost, I thanked Allah the Almighty for His blessings and guidance throughout this final year. Not forgetting the family especially my parents, brothers and sisters, sincere gratitude for their love and continuous support.

I would like to thank to various people who willing to spend their precious time guiding me and helping me to make my final year project a success.

First of all, I would like to express my greatest gratitude to my Final Year Project Supervisor, **AP. Dr. Anita Bt Ramli**, who has tight and busy working schedule yet spend time on me to monitor my progress during the 2 semester final year project. Her passion and communication skills in work and teaching really inspire me. I am also deeply grateful for her advice, patience and encouragement throughout my final year project duration.

Warmest gratitude to **Mr. Ahmad Shamil** (laboratory technician Block P), **Ms. Mas Fatiha** (Research Officer), other research officers and laboratory technicians Building 3, 4, 5 and 17 for their guidance, attention and time. I am benefited from their professional and personal advice. Thank you for your advice and relentless help regarding my final year project and study.

In addition, I would also like to give thanks to my internal examiner, **AP. Dr. Noor Asmawati Bt Mohd Zabidi**, **Prof. Dr. Khairun Azizi Bt Azizli** and **Dr. Moulay Rachid Babaa** for their constructive advices and recommendations.

Finally, I would like to thank any respective lecturers and my colleagues particularly UTP students who have directly or indirectly contributed to this project especially for their help, guidance, support, encouragement and warm friendship.

## TABLE OF CONTENTS

<b>CERTIFICATION OF APPROVAL</b>	.	.	.	.	.	.	.	<b>I</b>
<b>CERTIFICATION OF ORIGINALITY</b>	.	.	.	.	.	.	.	<b>II</b>
<b>ABSTRACT</b>	.	.	.	.	.	.	.	<b>III</b>
<b>ACKNOWLEDGEMENTS</b>	.	.	.	.	.	.	.	<b>IV</b>
<b>TABLE OF CONTENTS</b>	.	.	.	.	.	.	.	<b>V</b>
<b>LIST OF FIGURES AND TABLES</b>	.	.	.	.	.	.	.	<b>VII</b>
<b>LIST OF ABBREVIATIONS</b>	.	.	.	.	.	.	.	<b>IX</b>
<b>CHAPTER 1: INTRODUCTION</b>	.	.	.	.	.	.	.	<b>1</b>
<b>CHAPTER 2: LITERATURE REVIEW</b>	.	.	.	.	.	.	.	<b>4</b>
<b>CHAPTER 3: METHODOLOGY</b>	.	.	.	.	.	.	.	<b>11</b>
3.1 Catalyst Preparation	.	.	.	.	.	.	.	<b>11</b>
3.2 X-Ray Diffraction	.	.	.	.	.	.	.	<b>13</b>
3.3 Scanning Electron Microscopy	.	.	.	.	.	.	.	<b>13</b>
3.4 BET Surface Area Measurements	.	.	.	.	.	.	.	<b>13</b>
3.5 Flow Chart	.	.	.	.	.	.	.	<b>13</b>
3.5.1 Single-metal Catalyst	.	.	.	.	.	.	.	<b>13</b>
3.5.2 Bi-metal Catalyst (Sequential Method)	.	.	.	.	.	.	.	<b>14</b>
3.5.3 Co-impregnation Method	.	.	.	.	.	.	.	<b>14</b>
3.6 Project Gantt Chart	.	.	.	.	.	.	.	<b>15</b>
3.7 Tools, Equipments and Hardware	.	.	.	.	.	.	.	<b>16</b>

3.8	List of Chemicals	.	.	.	.	16
<b>CHAPTER 4:</b>	<b>RESULT AND DISCUSSION</b>	.	.	.	.	<b>17</b>
4.1	Data Gathering and Analysis of					
	Experimental Work	.	.	.	.	<b>18</b>
4.1.1	XRD Result	.	.	.	.	<b>18</b>
4.1.2	SEM Result	.	.	.	.	<b>20</b>
4.1.3	BET Result	.	.	.	.	<b>22</b>
4.2	Discussion on the Obtained Result	.	.	.	.	<b>27</b>
<b>CHAPTER 5:</b>	<b>CONCLUSION AND RECOMMENDATION</b>	.	.	.	.	<b>34</b>
5.1	Conclusion	.	.	.	.	<b>34</b>
5.2	Recommendation	.	.	.	.	<b>34</b>
<b>REFERENCES</b>	.	.	.	.	.	<b>35</b>
<b>APPENDICES</b>	.	.	.	.	.	<b>37</b>

## **LIST OF FIGURES**

- Figure 1                      Reaction Pathways of Ethanol Steam Reforming
- Figure 2                      List of Ethanol Steam Reforming using Noble Metal Catalyst
- Figure 3                      List of Ethanol Steam Reforming using Non-Noble Metal Catalyst
- Figure 4                      Catalytic Activities of Co-based Catalysts on Steam Reforming of Ethanol
- Figure 5                      Catalytic Activities of Fe Loaded Co/SrTiO<sub>3</sub> Catalysts on Steam Reforming of Ethanol
- Figure 6                      TEM Photographs for; Left: Co/SrTiO<sub>3</sub> and right: Fe/Co/SrTiO<sub>3</sub>
- Figure 7                      Flow chart of catalyst preparation and characterization for single metal catalyst
- Figure 8                      Flow chart of catalyst preparation and characterization for bi-metal catalyst (sequential method)
- Figure 9                      Flow chart of catalyst preparation and characterization for co-impregnation method
- Figure 10                     Process flow Gantt chart
- Figure 11                     XRD Pattern for Al<sub>2</sub>O<sub>3</sub>
- Figure 12                     XRD Pattern for Fe/Al<sub>2</sub>O<sub>3</sub> and Co-Fe/Al<sub>2</sub>O<sub>3</sub>
- Figure 13                     XRD Pattern for Co/Al<sub>2</sub>O<sub>3</sub>, Ratio Co:Fe=1:4 and Ratio Co:Fe=4:1
- Figure 14                     SEM photograph for Fe/Al<sub>2</sub>O<sub>3</sub>
- Figure 15                     SEM photograph for Co-Fe/Al<sub>2</sub>O<sub>3</sub> (sequential)
- Figure 16                     SEM photograph for Fe-Co/Al<sub>2</sub>O<sub>3</sub> (sequential)



- Figure 17 SEM photograph for Co-Fe/Al<sub>2</sub>O<sub>3</sub> (co-impregnation method)
- Figure 18 Isotherm Linear Plot for Al<sub>2</sub>O<sub>3</sub>
- Figure 19 Isotherm Linear Plot for Co/Al<sub>2</sub>O<sub>3</sub>
- Figure 20 Isotherm Linear Plot for Fe/Al<sub>2</sub>O<sub>3</sub>
- Figure 21 Isotherm Linear Plot for Co-Fe/Al<sub>2</sub>O<sub>3</sub> (sequential)
- Figure 22 Isotherm Linear Plot for Fe-Co/Al<sub>2</sub>O<sub>3</sub> (sequential)
- Figure 23 Isotherm Linear Plot for Al<sub>2</sub>O<sub>3</sub> (co-impregnation)
- Figure 24 SEM Photograph for  $\alpha$ -Al<sub>2</sub>O<sub>3</sub>
- Figure 25 Classification of Isotherms According to the BET Theory
- Figure 26 Hysteresis Loops on Type IV Isotherms
- Figure 27 XRD pattern for Fe/Al<sub>2</sub>O<sub>3</sub>
- Figure 28 XRD pattern for Co-Fe/Al<sub>2</sub>O<sub>3</sub> (sequential)
- Figure 29 XRD pattern for Fe-Co/Al<sub>2</sub>O<sub>3</sub> (sequential)
- Figure 30 XRD pattern for Co-Fe/Al<sub>2</sub>O<sub>3</sub> (co-impregnation method)
- Figure 31 XRD pattern for Co/Al<sub>2</sub>O<sub>3</sub>
- Figure 32 XRD Pattern for Co-Fe/Al<sub>2</sub>O<sub>3</sub> for Ratio Co:Fe=1:4
- Figure 33 XRD Pattern for Co-Fe/Al<sub>2</sub>O<sub>3</sub> for Ratio Co:Fe=4:1
- Figure 34 XRD Pattern for  $\alpha$ -Alumina and  $\gamma$ -Alumina
- Figure 35 XRD Pattern of supported CeO<sub>2</sub> and YDC. Samples: (a) Ce<sub>(10)</sub>/ $\gamma$  alumina, (b) 5YDC/ $\gamma$ -alumina, (c) 10YDC/ $\gamma$ -alumina

## LIST OF TABLES

Table 1	Tools, equipments and hardware involved
Table 2	List of Chemicals Involved
Table 3	Catalyst Composition
Table 4	Surface Area, Pore Volume and Pore Size for Al <sub>2</sub> O <sub>3</sub>
Table 5	Surface Area for Co/Al <sub>2</sub> O <sub>3</sub> , Fe/Al <sub>2</sub> O <sub>3</sub> and Co-Fe/Al <sub>2</sub> O <sub>3</sub>
Table 6	Pore Volume for Co/Al <sub>2</sub> O <sub>3</sub> , Fe/Al <sub>2</sub> O <sub>3</sub> and Co-Fe/Al <sub>2</sub> O <sub>3</sub>
Table 7	Pore Size for Co/Al <sub>2</sub> O <sub>3</sub> , Fe/Al <sub>2</sub> O <sub>3</sub> and Co-Fe/Al <sub>2</sub> O <sub>3</sub>
Table 8	BET Surface Area with Different Co Loading
Table 9	Properties of Cobalt and Ferum

## LIST OF ABBREVIATIONS

C <sub>2</sub> H <sub>5</sub> OH	Ethanol
H <sub>2</sub>	Hydrogen
CO <sub>2</sub>	Carbon Dioxide
Co	Cobalt
Fe	Iron
Al <sub>2</sub> O <sub>3</sub>	Aluminum Oxide
CO	Carbon Monoxide
SEM	Scanning Electron Microscopy
XRD	X-Ray Diffraction
Co(NO <sub>3</sub> ) <sub>2</sub> ·6(H <sub>2</sub> O)	Cobalt (II) Nitrate Hexahydrate
Fe(NO <sub>3</sub> ) <sub>3</sub> ·9H <sub>2</sub> O	Iron Nitrate Nonahydrate

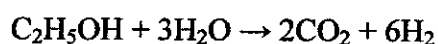
Ti	Titanium
Zr	Zirconium
Cr	Chromium
Mn	Manganese
Ni	Nickel
Cu	Copper
Zn	Zinc
Cd	Cadmium
Sb	Antimony
Ru	Ruthenium
Pt	Platinum
Rh	Rhodium

## CHAPTER 1

### INTRODUCTION

The process of steam reforming of hydrocarbons was developed in 1924 (Rostrup- Nielsen, 1984), is the main industrial method for production of hydrogen. Hydrogen is foreseen as a clean energy carrier in relation with the rapid development of fuel cell technologies. Indeed, its use in a fuel cell produces electricity and heat, with only water as a by-product. However, hydrogen is presently produced essentially from fossil hydrocarbons and only marginally by water electrolysis. Because of the depletion of world's fossil fuel reserves, the continual price rising and the serious environmental problems have turned more attention focusing on hydrogen production from renewable energy sources. The use of biomass as a hydrogen source has recently drawn attention as it is abundant worldwide and renewable, whereas its utilization has a near-zero CO<sub>2</sub> impact on the carbon life cycle. Besides produced clean energy, they will not run out by rational utilization. Hydrogen production such as from biomass sources can reduce the emissions of sulfur and nitric oxide content and also the neutral energy of Carbon Dioxide supply can be achieved, so it's an environment friendly process.

Among the various feedstocks, ethanol is a very promising candidate as it has relatively high hydrogen content, availability, non toxicity, storage and handling safety. If ethanol reacts in a most desirable way, the reaction is as follow:



Basically, steam reforming of ethanol to produce only H<sub>2</sub> and CO<sub>2</sub> favors at high temperatures, while by- product formation is rather dominant at low temperatures. The amount of hydrogen produced also larger than that accompanied by by- product formation at lower temperatures. However, in term of energy saving, low temperature reaction accompanied with the formation of useful by- products is preferable.

The aim of the steam reforming of ethanol is to obtain the hydrogen with high activity, selectivity and stability. Although hydrogen can be produced by direct gasification of solid biomass, the catalysts poisoning by liquid tars and solid chars formed during the process remains a major issue. The wide variety of biomass sources (energy crops, agricultural and forest residues, industrial and municipal waste, etc.) can differ considerably in composition (poisoning compounds, ashes) and moisture content, which implies adapting the process and the catalyst to the feed. Thus, steam reforming process is selected since the hydrogen yield is higher. To this purpose, selection of catalyst is seems to be a crucial part as it plays a role in the reactivity toward complete conversion of ethanol. In this paper, Co-Fe/Al<sub>2</sub>O<sub>3</sub> is chosen to be a catalyst for steam reforming process. The combination of Cobalt and Iron gives high stabilizing oxide, longer lifetime and resulted as active metal. Cobalt is one of the non-noble metal catalysts as supported Co could break the C-C bond [1]. On heating, it decomposes to respective oxides which is Cobalt Oxides then reduced to the active metal. Recent works provide that Co/Al<sub>2</sub>O<sub>3</sub> gives high catalytic activity and selectivity to hydrogen. However, coke formations on the catalysts are detected after 9 hours of this process at 400°C. To minimize coking and catalyst deactivation, coke precursor gasification and steam activation over the catalyst are to be facilitated.

There are various methods to prepare the catalyst for steam reforming process. Proper selection of methods should be taken into a consideration as the objective to achieve high production of hydrogen. Thus, in this project, the catalyst was prepared using incipient wetness method since it is the simplest method when using porous support metal catalyst. Typically, the active metal precursor is dissolved in an aqueous or organic solution. Then the metal-containing solution is added to a catalyst support containing the same pore volume as the volume of solution that was added. By having similar parameters such as operating temperature and pressure, sequential impregnation and co- impregnation method were carried out throughout this project in order to determine which method can give high hydrogen production. Different molar ratio between Co and Fe in the samples also being investigated to indicate which metal contributes more toward the process.

The characterization of catalyst was done using X-Ray Diffraction (XRD), Scanning Electron Microscopy (SEM) and Brunauer-Emmett-Teller (BET). From XRD pattern, the crystalline phase is analyzed and the peak of intensity is being study. With high magnification of image, SEM presented the morphology of metal coating on the surface of support catalyst. The SEM micrographs indicate that the alumina is crystalline with a well- defined plane exposed and that both metals coated on the support surface uniformly. While for BET, the catalyst surface area and dispersion are shown as functions of metal loading for the various series of impregnation and ratio. Each of the techniques utilized provides a particular but different type of information about this complex industrial catalyst. The information is complimentary and when combined yields a detailed understanding of the morphology, composition and chemical nature of  $\alpha$ - $\text{Al}_2\text{O}_3$ - supported Co and Fe.

The project has been determined to be feasible enough within the areas of study. Fundamental of steam reforming process is studied as to get the clear picture of this operation and being aware of the important parameters involved. There are many available and possible catalysts to be used for this process. Thus, the proper selection of catalyst is a crucial task as to get the most suitable metals for this process. The duration for the preparation and characterization of the catalyst is determined to be feasible within the time frame given since the method used manages to produce a sample less than a week regardless of the equipment failure. From the estimated calculation, the preparation of the catalyst can be done within the two to three weeks then followed by the characterization process and hydrogen testing. All the procedures involved will be done step by step accordingly to ensure this project is lies within the timeline.

In the following chapter, the literature review and the theory for preparation and characterization of catalyst for steam reforming of ethanol will be discussed. Brief description about the procedure and detail explanation for every result obtained will be covered through the methodology followed by result and recommendation section. The relevancy of the objectives will be seen throughout this project together with possible future work for expansion and continuation.

## CHAPTER 2

### LITERATURE REVIEW

The demand for hydrogen has been increasing during the past years due to the need to reduce the sulfur content in fuels. Hydrogen production from steam reforming is non-toxicity, safe storage and handling. It is a renewable fuel, which does not contribute to an increase in the Earth's greenhouse effect. Thus, the production of hydrogen has become relevant in both economic and social terms, as it related to quality of life.

Biomass has become an alternative energy resource to fossil fuels. In ethanol production, much water coexists after fermentation process. In order to use ethanol as to substitute for gasoline, this water must be removed completely. Steam reforming of ethanol generates a hydrogen-rich-high-calorie gas without rectification. The hydrogen production is available for multipurpose such as use in fuel cells.

Figure below shows the reaction pathways and thermodynamics of ethanol steam reforming [2]. It can be seen that hydrogen production varies significantly with different reaction pathways.

*Figure 1: Reaction Pathways of Ethanol Steam Reforming*

Reaction	Equation	Remarks
Sufficient steam supply	$C_2H_5OH + 3H_2O \rightarrow 2CO_2 + 6H_2$	Ideal pathway, the highest hydrogen production
Insufficient steam supply	$C_2H_5OH + H_2O \rightarrow 2CO + 4H_2$ $C_2H_5OH + 2H_2 \rightarrow 2CH_4 + H_2O$	Undesirable products, lower hydrogen production
Dehydrogenation	$C_2H_5OH \rightarrow C_2H_4O + H_2$	Reaction pathways for hydrogen production in practice
Acetaldehyde decomposition	$C_2H_4O \rightarrow CH_4 + CO$	
Acetaldehyde steam reforming	$C_2H_4O + H_2O \rightarrow 3H_2 + 2CO$	Undesired pathway, main source of coke formation
Dehydration	$C_2H_5OH \rightarrow C_2H_4 + H_2O$	
Coke formation	$C_2H_4 \rightarrow$ polymeric deposits (coke)	Coke formation, low hydrogen production
Decomposition	$C_2H_5OH \rightarrow CO + CH_4 + H_2$	
	$2C_2H_5OH \rightarrow C_2H_6O + CO + 3H_2$ $C_2H_5OH \rightarrow 0.5CO_2 + 1.5CH_4$	
Reaction of decomposition products		
Methanation	$CO + 3H_2 \rightarrow CH_4 + H_2O$ $CO_2 + 4H_2 \rightarrow CH_4 + 2H_2O$	
Methane decomposition	$CH_4 \rightarrow 2H_2 + C$	
Boudouard reaction	$2CO \rightarrow CO_2 + C$	
Water gas shift reaction (WGSR)	$CO + H_2O \rightarrow CO_2 + H_2$	Reduce coke formation, enhance hydrogen production

In the ethanol reforming process, beside formation of H<sub>2</sub>, CO<sub>2</sub>, H<sub>2</sub>O and CH<sub>4</sub>, the gaseous fuel produced usually contains high levels of CO [3]. Thus, it is crucial to ensure the hydrogen dehydration and decomposition is minimized to avoid the coke formation. From previous reaction path analysis, coke formation is mainly caused Boudouard reaction, polymerization of ethylene or by decomposition of methane formed during ethanol steam reforming. Coke can destroyed catalyst structure and occupy catalyst surface, thus considerably reduce catalyst activity. Coke formation is faster on acidic support as dehydration occurs. This adverse effect can be reduced by using basic oxide as support or adding alkali species onto the acidic support.

Catalysts are substances that change the reaction rate by promoting a different mechanism for the reaction without being consumed in the reaction. As they decrease the activation energy barrier of the reaction, from the principle of microkinetic reversibility, they also decrease the activation energy barrier for the reverse of that reaction. In this respect, it may be expected for a good higher alcohol synthesis catalyst also to be a good steam reforming catalyst. Active catalysts should maximize hydrogen selectivity and inhibit coke formation as well as CO production. Generally, there are two groups of catalyst which are noble metal and non-noble metal catalysts [2]. List of possible catalysts and their support is summarized below:

*Figure 2: List of Ethanol Steam Reforming using Noble Metal Catalyst*

Catalyst	Support	Temperature (K)	Steam/Ethanol molar ratio	Ethanol conversion (%)	Hydrogen selectivity (%)	Reference
Rh (1 wt%) (2 wt%)	$\gamma$ -Al <sub>2</sub> O <sub>3</sub>	1073	3:1	100 100	~ 95 ~ 96	[14]
Ru (1 wt%) (5 wt%)				42 100	~ 55 ~ 96	
Rt (1 wt%) Pd (1 wt%)				60 55	~ 65 ~ 50	
Rh (5 wt%)	$\gamma$ -Al <sub>2</sub> O <sub>3</sub>		8.4:1	100% at the beginning 43% 100h after operation	Unknown	[15]
Rh (3 wt%) Pt (3 wt%) Ni (21 wt%) Co (21 wt%)	MgO	923	8.5:1	99 (10h) 10 (10h) 42 (10h) 55 (10h)	91 70 97 92	[17]
Ru (1 wt%) Rh (1 wt%)	CeO <sub>2</sub>	723	Not known	Above 90%	57 (20 min) 25 (100 min) 82 (20 min) 56 (80 min)	[18]
Rh (2 wt%)	CeO <sub>2</sub>	573 673 723	8:1	58.5 100 100	59.7 66.3 69.1	[22]
	ZrO <sub>2</sub>	573 723		100 100	57.4 70.3	



**Figure 3: List of Ethanol Steam Reforming over Non- Noble Metal Catalyst**

Catalyst	Support	Temperature (K)	Steam/ethanol molar ratio	Ethanol conversion (%)	Hydrogen selectivity (%)	Reference	
Ni (20 wt%)	La <sub>2</sub> O <sub>3</sub>	773	3:1	35	70	[13]	
		1073		~ 100	95		
	$\gamma$ -Al <sub>2</sub> O <sub>3</sub>	973		77	87		
		1073		100	96		
Ni (20.6 wt%)	Y <sub>2</sub> O <sub>3</sub>	523	3:1	81.9	43.1	[23]	
Ni (16.1 wt%)	$\gamma$ -Al <sub>2</sub> O <sub>3</sub>			76	44		
Ni (15.3 wt%)	La <sub>2</sub> O <sub>3</sub>			80.7	49.5		
Ni (35 wt%)	$\gamma$ -Al <sub>2</sub> O <sub>3</sub>	773	6:1	100	91	[24]	
Ni (3.8 wt%)	Al <sub>2</sub> O <sub>3</sub> (heat treatment at 823 K)	723	3:1	96.6	61.5	[28]	
		923		100	89.0		
	Al <sub>2</sub> O <sub>3</sub> (heat treatment at 973 K)	723		100	0		
		823		99.2	67.3		
		923		100	87.4		
Ni (10 wt%)	$\gamma$ -Al <sub>2</sub> O <sub>3</sub>	923	8:1	100	78.2	[29]	
	MgO			100	82.2		
	La <sub>2</sub> O <sub>3</sub>			100	89.3		
	ZnO			100	89.1		
Co (10 wt%)	ZnO	623	4:1	100	73.4	[38]	
Co (10 wt%), addition with Na	ZnO	673	13:1	(75 h)		[39]	
				Na (0.06 wt%)	100		72.1
				Na (0.23 wt%)	100		73.4
				Na (0.78 wt%)	100		74.2
Co (8 wt%)	Al <sub>2</sub> O <sub>3</sub>	673	3:1	74	60-70	[41]	
				(18 wt%)	99		63-70
	(8 wt%)			89	62-70		
(18 wt%)	SiO <sub>2</sub>			97	69-72		

Supports also play important roles in steam reforming of ethanol, as supports help in the dispersion of metal catalyst and may enhance metal catalyst activity via metal-support interactions. Support may promote migration of OH group toward the metal catalyst in the presence of water at high temperature, facilitating steam reforming reactions [4]. Al<sub>2</sub>O<sub>3</sub> is commercial supports because all practical industrial ethanol synthesis catalysts are supported with alumina. They increase the surface area and stability of the catalyst and therefore, they are structural promoters. They also induce the formation of side products and hydrocarbons. However, due to its acidic nature, Al<sub>2</sub>O<sub>3</sub> induces dehydration of ethanol, leading to coke formation. Addition of alkali species can improve catalyst stability as its acidity can be partly neutralized. Thus, the selection of support can significantly inhibit ethanol dehydration, greatly reducing coke formation. Catalyst supports not only can effect reaction pathways, but also can effect metal dispersion and inhibit metal sintering.

$\text{Al}_2\text{O}_3$  was reported to have the highest selectivity for steam reforming of ethanol by suppression of methanation and decomposition of ethanol [5, 7]. The selectivity of  $\text{H}_2$  decreased in the order:  $\text{Co}/\text{Al}_2\text{O}_3 > \text{Co}/\text{ZrO}_2 > \text{Co}/\text{MgO} > \text{Co}/\text{SiO}_2 > \text{Co}/\text{C}$ . Due to the basic characteristics of  $\text{MgO}$ ,  $\text{Co}/\text{MgO}$  was more resistant to coke formation than that of  $\text{Co}/\text{Al}_2\text{O}_3$  at 923K.

$\text{Co}/\text{Al}_2\text{O}_3$  (8.6 wt%),  $\text{Co}/\text{SiO}_2$  (7.8 wt%) and  $\text{Co}/\text{MgO}$  (18 wt%), prepared by impregnation method, all showed high catalytic activity (>90% ethanol conversion) and selectivity to hydrogen (about 70%). However, after 9 hours of steam reforming at 673K, coke formation on the catalysts were detected in the following decreasing order:  $\text{Co}/\text{Al}_2\text{O}_3$  (24.6 wt% coke) >  $\text{Co}/\text{MgO}$  (17 wt% coke) >  $\text{Co}/\text{SiO}_2$  (14.2 wt% coke). The highest coke formation on alumina was ascribed to the acidic character of alumina, which favored ethanol dehydration to ethylene. Their subsequent study showed that CO in the outlet gas stream could be reduced by increasing the cobalt content. Despite their comparable selectivity to hydrogen,  $\text{Co}/\text{Al}_2\text{O}_3$  showed higher efficiency for CO removal.

To increase the catalyst activity, many promoters have been investigated for Co catalysts. These promoters has been identified can increase the reducibility of Co, preserve the activity by preventing the formation of coke, exhibit cluster and ligand effects, act as a source of hydrogen spillover and enhance the dispersion. It has been found that metal dispersion, chemical state, as well as catalyst activity are affected by changing the interaction between the metal catalytic phase and the support [6].

The higher activity catalyst was detected by addition of a small amount of Fe on  $\text{Co}/\text{SrTiO}_3$ , which had high activity [7]. It was found that Fe loading promoted the  $\text{Co}/\text{SrTiO}_3$  activity. Effect of Fe loading was examined by changing the amount of Fe loading. List below are the comparison on catalytic activity with and without addition of Fe. It is consider that Fe-loaded catalysts suppress decomposition of  $\text{CH}_3\text{CHO}$  and promote selective reaction to steam reforming of ethanol.

**Figure 4: Catalytic Activities of Co-based Catalysts on Steam Reforming of Ethanol**

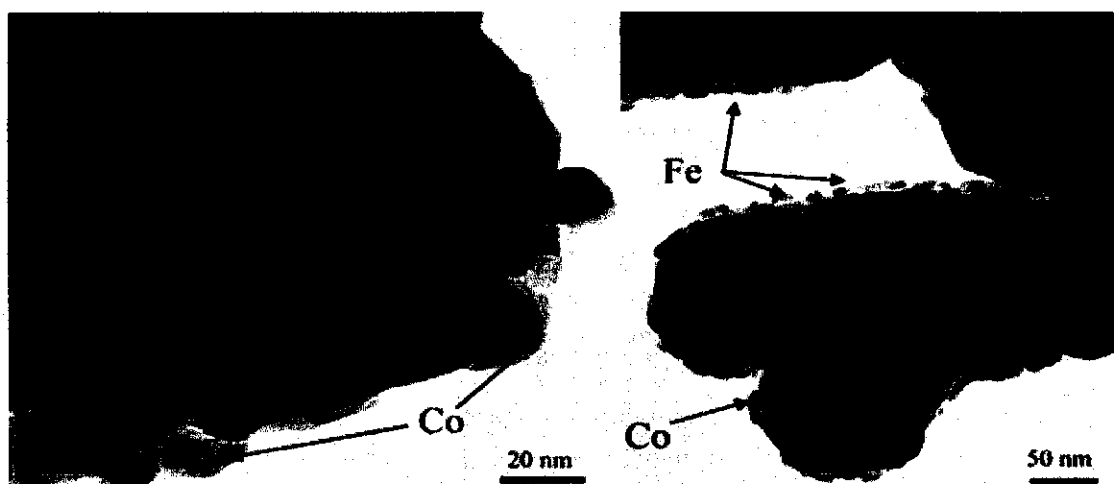
Catalyst	Selectivity (%)				Ethanol conversion (%)	H <sub>2</sub> yield (%)	r <sub>H</sub> /r <sub>D</sub>
	CH <sub>3</sub> CHO	CO	CO <sub>2</sub>	CH <sub>4</sub>			
Co/SrTiO <sub>3</sub>	22.6	14.8	53.9	7.0	70.2	96.8	8.8
Pt/Co/SrTiO <sub>3</sub>	7.6	9.3	55.8	27.0	89.8	95.3	1.4
Pd/Co/SrTiO <sub>3</sub>	8.2	13.2	60.5	17.5	83.0	109.0	3.2
Rh/Co/SrTiO <sub>3</sub>	2.1	11.4	64.4	22.1	95.4	136.0	2.4
Cr/Co/SrTiO <sub>3</sub>	22.7	16.8	52.0	6.8	65.1	87.5	9.1
Cu/Co/SrTiO <sub>3</sub>	35.2	19.2	35.7	6.5	77.9	76.3	7.4
Fe/Co/SrTiO <sub>3</sub>	12.7	22.3	60.8	3.5	81.1	133.0	23.1

**Figure 5: Catalytic Activities of Fe Loaded Co/SrTiO<sub>3</sub> Catalysts on Steam Reforming of Ethanol**

Fe loading (mol%)	Selectivity (%)				Ethanol conv. (%)	H <sub>2</sub> yield (%)	r <sub>H</sub> /r <sub>D</sub> ratio (-)
	CH <sub>3</sub> CHO	CO	CO <sub>2</sub>	CH <sub>4</sub>			
0	22.6	14.8	53.9	7.0	70.2	96.8	8.8
0.10	14.1	14.7	65.0	4.9	71.4	120.2	15.3
0.33	13.0	18.8	62.9	4.6	80.4	132.9	16.8
0.65	12.7	22.3	60.8	3.5	81.1	133.0	23.1
0.98	16.6	34.2	43.6	4.5	85.2	126.8	16.3
1.3	13.9	41.3	40.4	3.0	85.2	126.3	26.2
2.6	20.6	47.9	23.9	3.6	72.2	91.9	18.9

As presented above, selectivity of CO was raised by the increase of additive amount of Fe and selectivity to CH<sub>4</sub> was decreased by addition of Fe. Addition of Fe suppressed the decomposition of acetaldehyde to form methane and also it suppressed water gas shift reaction. Furthermore, the maximum value existed with C<sub>2</sub>H<sub>5</sub>OH conversion and H<sub>2</sub> yield when the Fe loading amount was changed. Higher H<sub>2</sub> yield obtained with Fe/Co/SrTiO<sub>3</sub> catalyst comes from the higher reforming activity of CH<sub>3</sub>CHO and not from the WGS activity. From the viewpoint of hydrogen production, Fe loading of between 0.33 and 1.30% was very effective. This window of 0.33-1.30 mol% is close to the amount at which Fe is added as an atomic monolayer onto Co/SrTiO<sub>3</sub>. Figure below shows the TEM photograph for the catalyst before/after the second impregnation of Fe on Co/SrTiO<sub>3</sub>.

Figure 6: TEM Photographs for; Left: Co/SrTiO<sub>3</sub> and right: Fe/Co/SrTiO<sub>3</sub>



Before the second impregnation of Fe, the diameter of Co particle was about 20nm and after the second impregnation of Fe, very small grains of Fe (much smaller than Co particle) can be found on the catalyst. So these small particles of Fe played an important role on the promoting effect to the steam reforming of ethanol/acetaldehyde. Thus, the Fe-modified Co/SrTiO<sub>3</sub> catalyst showed a stable high activity and the highest selectivity to steam reforming, with low carbon deposits. Therefore, interaction among Fe, Co and SrTiO<sub>3</sub> perovskite seems to serve an important role for high activity and hydrogen selectivity over Fe/Co/SrTiO<sub>3</sub> catalyst during steam reforming of ethanol.

Over 40 years, Ni has widely used as a catalyst in reforming process. From a practical and a fundamental point of view, there are four challenges for Ni steam reforming catalysts which are activity, sulfur poisoning, carbon formation and sintering [8]. For activity, the catalyst must have sufficient activity to equilibrate the reaction mixture in the design catalyst volume. Sulfur is a strong poison for Ni catalysts and will blocks the active Ni sites. In the carbon formation, it may increase the pressure drop, crush the catalyst pellets, block the active Ni surface and even form at the inner perimeter of the reforming tubes resulting in a lower heat transfer. Sintering refers to the growing of catalysts during operation. Sintering influences the three other challenges so it is important in steam reforming due to high temperatures and high pressures of steam.

There are many ways to prepare the catalyst for steam reforming process. For the impregnation method, this procedure requires that the support is contacted with a certain amount of solution of the metal precursor, usually a salt, and then it is aged, usually for a short time, dried and calcined. According to the amount of solution used, two types of impregnation can be distinguished, incipient wetness or dry impregnation. The incipient wetness method involves the use of an excess of solution with respect to the pore volume of the support [9]. The system is left to age for a certain time under stirring, filtered and dried. This procedure is applied especially when a precursor-support interaction can be envisaged. Therefore, the concentration of the metal precursors on the support will depend not only on the concentration of the solution and on the pore volume of the support, but also on the type and/or concentration of adsorbing sites existing at the surface.

Calcination has the purpose of decomposing the metal precursor with formation of an oxide and removal of gaseous products (usually water,  $\text{CO}_2$ ) and the cations or the anions which have been previously introduced. In the case of industrial production, calcinations is useful for the removal of extraneous materials, like binders or lubricants, which have been used during the previous forming operations (extrusion, tableting, etc.). Besides decomposition, during the calcinations, a sintering of the precursor or of the formed oxide and a reaction of the latter with the support can occur. In fact, in case of alumina as the support, a calcination performed at temperatures around 500-600°C, can give rise to reaction with divalent metal (Ni, Co, Cu) oxide with consequent formation on the surface of metal aluminates which are more stable than the oxides and so might require a higher temperature of reduction than that needed for the oxides. However, this is not a problem if the reduction temperature is not going to cause excessive sintering; in fact after reduction, the final catalysts will be well dispersed due to this textural effect. When dealing with bimetallic catalysts, a severe control of calcinations temperature is required in order to avoid the formation of two separate oxides or segregation of one of the component.

## CHAPTER 3

### METHODOLOGY

#### 3.1 Catalyst Preparation

There are 5 samples of catalyst were prepared in this project. The total weight of Co-Fe/Al<sub>2</sub>O<sub>3</sub> was set to be 50g where 2.5g of metal and 47.5g of supported catalyst (95%- supported catalyst and 5%- metal). The catalysts used in these experiments were all based upon  $\alpha$ -alumina and the metallic precursors were all in the form of nitrates. For the first sample, 12.3472g of Cobalt (II) Nitrate Hexahydrate, Co(NO<sub>3</sub>)<sub>2</sub>·6(H<sub>2</sub>O) was dissolved in sufficient quantity of deionized water. 47.5g of Al<sub>2</sub>O<sub>3</sub> was added to the Cobalt solution, stirred for 6 hours, dried at 120°C for 16 hours and calcined at 500°C for another 16 hours in the rotary furnace. Thus, the catalyst obtained was Co/Al<sub>2</sub>O<sub>3</sub>.

Same goes to the second sample whereby 18.0858g of Iron Nitrate, Fe(NO<sub>3</sub>)<sub>3</sub>·9H<sub>2</sub>O was dissolved in sufficient quantity of deionized water. 47.5g of Al<sub>2</sub>O<sub>3</sub> was added to the Iron solution, stirred for 6 hours, dried at 120°C for 16 hours and calcined at 500°C for another 16 hours in the rotary furnace. Thus, the catalyst obtained was Fe/Al<sub>2</sub>O<sub>3</sub>. Noted that for the first and second sample was single metal catalyst.

Next, the catalyst was prepared in the sequential method. For the third sample, 12.3472g of Cobalt (II) Nitrate Hexahydrate, Co(NO<sub>3</sub>)<sub>2</sub>·6(H<sub>2</sub>O) was dissolved in sufficient quantity of deionized water. 47.5g of Al<sub>2</sub>O<sub>3</sub> was added to the Cobalt solution, stirred for 6 hours, dried at 120°C for 16 hours and calcined at 500°C for another 16 hours in the rotary furnace. 47.5g of Co/Al<sub>2</sub>O<sub>3</sub> was added to an aqueous solution containing 18.0858g of Iron Nitrate, Fe(NO<sub>3</sub>)<sub>3</sub>·9H<sub>2</sub>O. The mixture was stirred for 6 hours, dried at 120°C for 16 hours and calcined at 500°C for another 16 hours in the rotary furnace. Thus, the catalyst obtained was Co-Fe/Al<sub>2</sub>O<sub>3</sub>.

For the fourth sample, 18.0858g of Iron Nitrate,  $\text{Fe}(\text{NO}_3)_3 \cdot 9\text{H}_2\text{O}$  was dissolved in sufficient quantity of deionized water. 47.5g of  $\text{Al}_2\text{O}_3$  was added to the Iron solution, stirred for 6 hours, dried at  $120^\circ\text{C}$  for 16 hours and calcined at  $500^\circ\text{C}$  for another 16 hours in the rotary furnace. 47.5g of  $\text{Fe}/\text{Al}_2\text{O}_3$  was added to an aqueous solution containing 12.3472g of Cobalt (II) Nitrate Hexahydrate,  $\text{Co}(\text{NO}_3)_2 \cdot 6(\text{H}_2\text{O})$ . The mixture was stirred for 6 hours, dried at  $120^\circ\text{C}$  for 16 hours and calcined at  $500^\circ\text{C}$  for another 16 hours in the rotary furnace. Thus, the catalyst obtained was  $\text{Fe-Co}/\text{Al}_2\text{O}_3$ .

Next, for the fifth sample, the catalyst was prepared by co-impregnation method whereby 45g of  $\text{Al}_2\text{O}_3$  was added to 12.3472g of an aqueous solution of Cobalt (II) Nitrate Hexahydrate,  $\text{Co}(\text{NO}_3)_2 \cdot 6(\text{H}_2\text{O})$  and 18.0858g of Iron Nitrate,  $\text{Fe}(\text{NO}_3)_3 \cdot 9\text{H}_2\text{O}$ . Note that there are 2.5g of Co in 12.3472g of  $\text{Co}(\text{NO}_3)_2 \cdot 6(\text{H}_2\text{O})$  and 2.5g of Fe in 18.0858g of  $\text{Fe}(\text{NO}_3)_3 \cdot 9\text{H}_2\text{O}$ . The mixture was stirred for 6 hours, dried at  $120^\circ\text{C}$  for 16 hours and calcined at  $500^\circ\text{C}$  for another 16 hours in the rotary furnace. Thus, the catalyst obtained was  $\text{Co-Fe}/\text{Al}_2\text{O}_3$ . Noted that for the third, fourth and fifth sample were bi-metal catalyst.

In the co-impregnation method, both metals were prepared in equal weight, 2.5g each. Instead of same ratio, the catalyst also was prepared using ratio 1:4 and 4:1. Thus, for the sixth sample, with the ratio of  $\text{Co:Fe} = 1:4$ , 45g of  $\text{Al}_2\text{O}_3$  was added to 4.9386g of an aqueous solution of Cobalt (II) Nitrate Hexahydrate,  $\text{Co}(\text{NO}_3)_2 \cdot 6(\text{H}_2\text{O})$  and 28.8571g of Iron Nitrate,  $\text{Fe}(\text{NO}_3)_3 \cdot 9\text{H}_2\text{O}$ . The mixture was stirred for 6 hours, dried at  $120^\circ\text{C}$  for 16 hours and calcined at  $500^\circ\text{C}$  for another 16 hours in the rotary furnace.

Last but not least, with the ratio of  $\text{Co:Fe} = 4:1$ , 45g of  $\text{Al}_2\text{O}_3$  was added to 19.7979g of an aqueous solution of Cobalt (II) Nitrate Hexahydrate,  $\text{Co}(\text{NO}_3)_2 \cdot 6(\text{H}_2\text{O})$  and 7.2343g of Iron Nitrate,  $\text{Fe}(\text{NO}_3)_3 \cdot 9\text{H}_2\text{O}$ . The mixture was stirred for 6 hours, dried at  $120^\circ\text{C}$  for 16 hours and calcined at  $500^\circ\text{C}$  for another 16 hours in the rotary furnace.

### 3.2 X-Ray Diffraction

X-ray powder diffraction was applied to identify the crystalline phases presented in the samples. The  $2\theta$  scale was used and the intensity of the peak was observed thoroughly.

### 3.3 Scanning Electron Microscopy

The catalyst samples were analyzed with the magnification of 5000-10 000. The pellets size was observed in the range of 100-200 nm and the morphology of the metal coated on the surface of support is being studied.

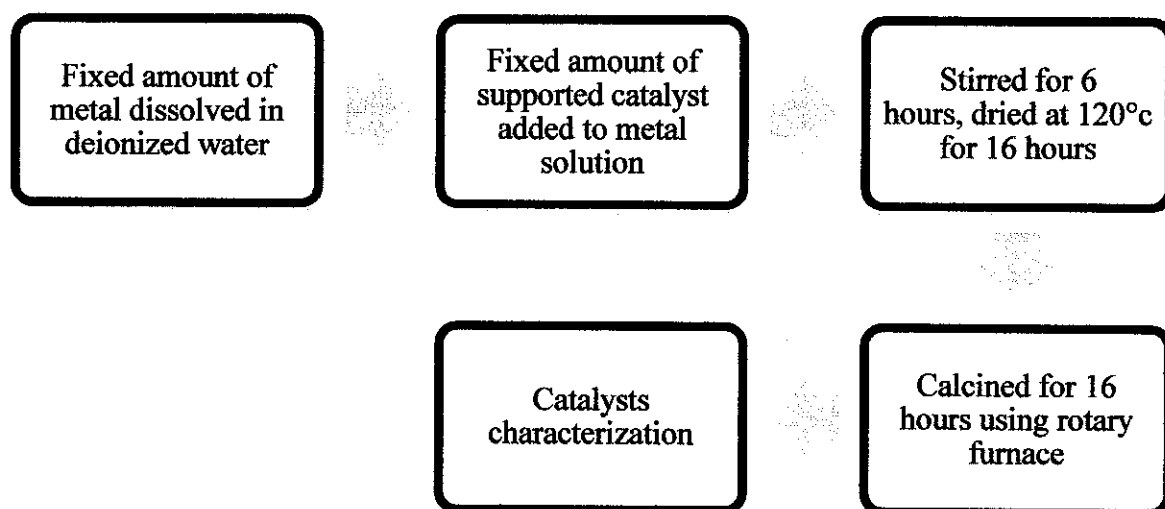
### 3.4 BET Surface Area Measurements

The specific surface area of the various samples was measured according to Brunauer-Emmet-Teller (BET) method by nitrogen adsorption. Prior to adsorption measurements, the samples were degassed for at least 12h at 250°C.

### 3.5 Flow Chart

#### 3.5.1 Single metal catalyst

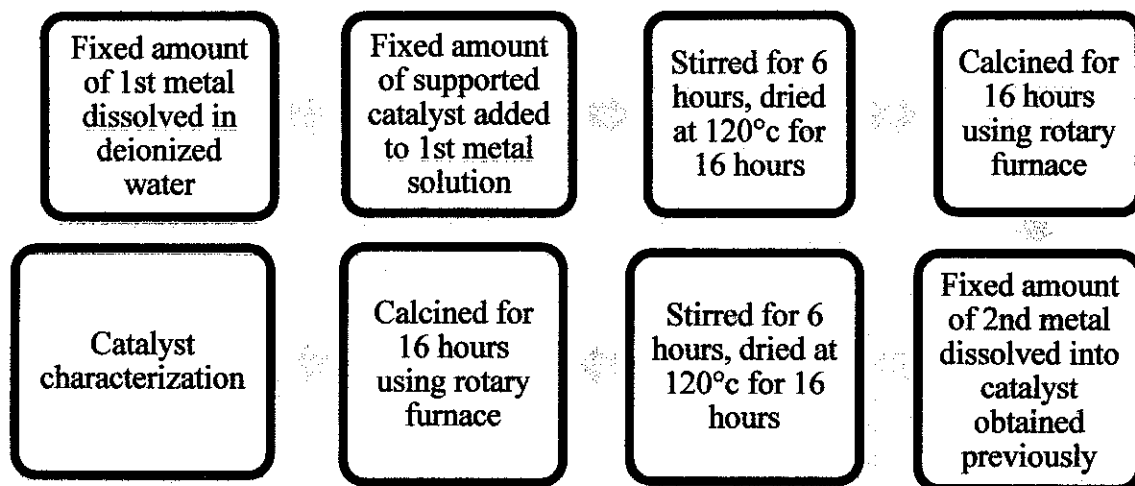
*Figure 7: Flow chart of catalyst preparation and characterization for single metal catalyst*





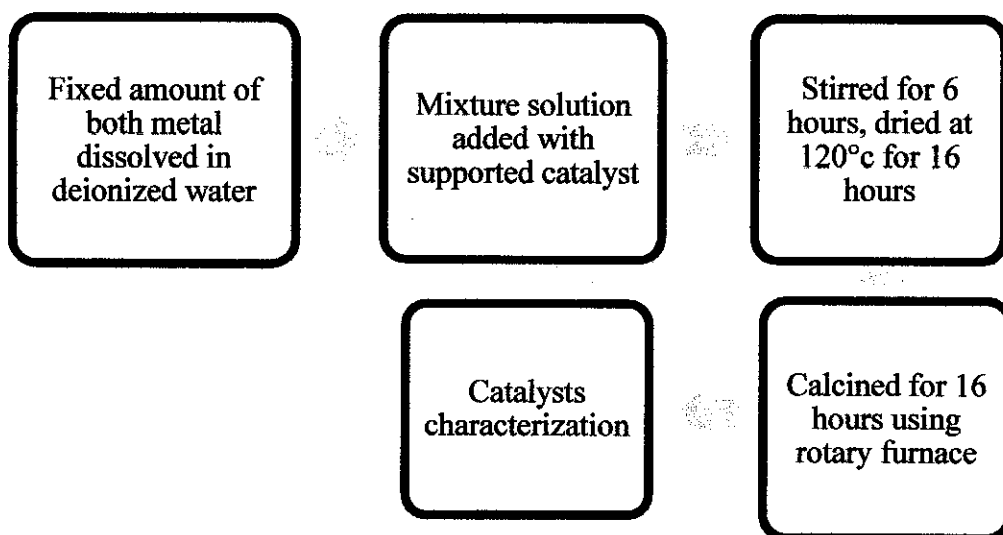
### 3.5.2 Bi-metal catalyst (sequential method)

Figure 8: Flow chart of catalyst preparation and characterization for bi-metal catalyst (sequential method)



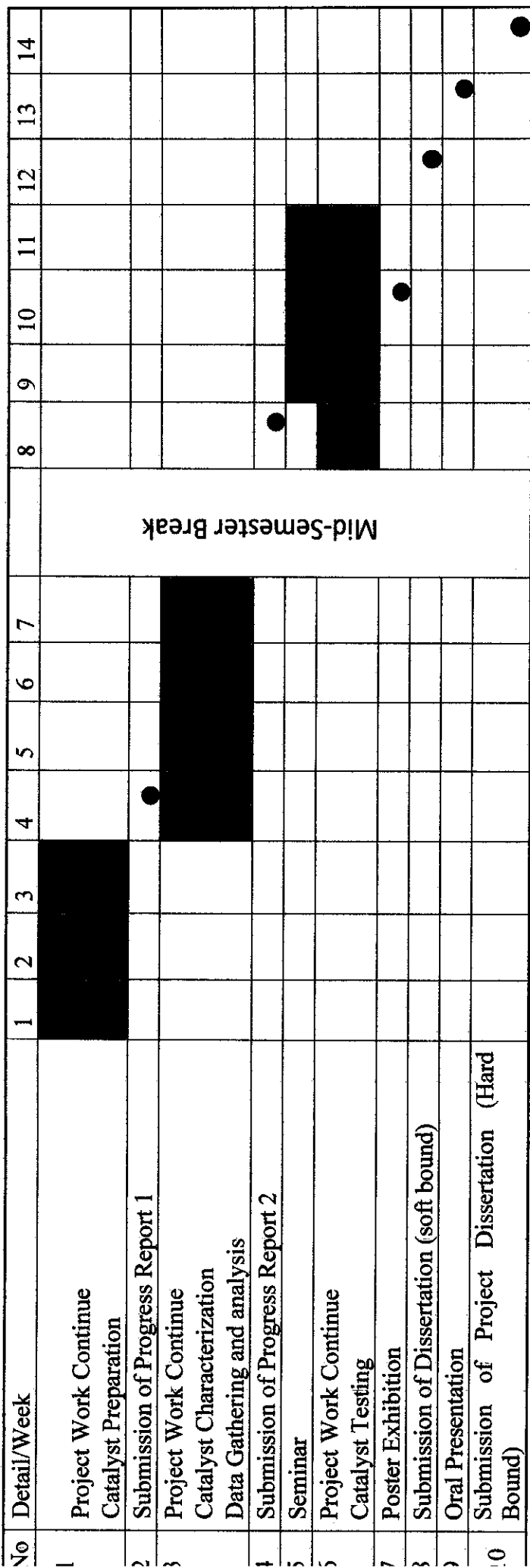
### 3.5.3 Co-impregnation method

Figure 9: Flow chart of catalyst preparation and characterization for co-impregnation method



### 3.6 Project Gantt Chart

Figure 10: Process flow Gantt chart



● Suggested Milestone

█ Process

### 3.7 Tools, Equipments and Hardware

*Table 1: Tools, equipments and hardware involved*

No	Tools, Equipments, Hardware	Function
1	Beaker 250ml, 500ml	To dissolve metal
2	Spatula	To transfer chemical
3	Crucible	To calcine Al <sub>2</sub> O <sub>3</sub>
4	Magnetic Stirrer	To stir solution
5	Furnace, Oven	To dry solution
6	Rotary furnace	To calcine catalyst
7	Reactor	Steam reforming of ethanol process

### 3.8 List of Chemicals

*Table 2: List of Chemicals Involved*

No	Details
1.	Name: Aluminium Oxide – Calcined Chemical Formula: Al <sub>2</sub> O <sub>3</sub> Molecular Weight: 101.96 Supplier: Fisher Scientific UK Limited
2.	Name: Iron Nitrate Nonahydrate Chemical Formula: Fe(NO <sub>3</sub> ) <sub>3</sub> .9H <sub>2</sub> O Molecular Weight: 404 Supplier: R&M Marketing, Essex, UK
3.	Name: Cobalt Nitrate Hexahydrate Chemical Formula: Co(NO <sub>3</sub> ) <sub>2</sub> .6H <sub>2</sub> O Molecular Weight: 291.04 Supplier: Merck KGaA, Germany

## CHAPTER 4

### RESULT AND DISCUSSION

For the catalyst preparation, it has been divided into two batches. The first batch of catalyst was prepared by varying the method and sequence. The support catalyst and single metal catalyst also include in this batch for the characterization and comparison purpose. While for the second batch, the catalyst was prepared by varying the ratio of precursors.

Both the first and second batch of catalyst has been successfully prepared. The catalysts with the percentages are as follow:

*Table 3: Catalyst Composition*

Catalyst	Weight Percentage (wt%)			Mass (g)			Remarks
	Al <sub>2</sub> O <sub>3</sub>	Cobalt	Ferum	Al <sub>2</sub> O <sub>3</sub>	Cobalt	Ferum	
Al <sub>2</sub> O <sub>3</sub>	100	-	-	50	-	-	
Co/Al <sub>2</sub> O <sub>3</sub>	95	5	-	47.5	2.5	-	
Fe/Al <sub>2</sub> O <sub>3</sub>	95	-	5	47.5	-	2.5	
Co-Fe/Al <sub>2</sub> O <sub>3</sub>	95	2.5	2.5	47.5	2.5	2.5	1 <sup>st</sup> Sequence (Co followed by Fe)
Fe-Co/Al <sub>2</sub> O <sub>3</sub>	95	2.5	2.5	47.5	2.5	2.5	2 <sup>nd</sup> Sequence (Fe followed by Co)
Co-Fe/Al <sub>2</sub> O <sub>3</sub>	95	2.5	2.5	45	2.5	2.5	Co-impregnation
Co-Fe/Al <sub>2</sub> O <sub>3</sub>	95	1	4	45	1	4	Co:Fe = 1:4
Co-Fe/Al <sub>2</sub> O <sub>3</sub>	95	4	1	45	4	1	Co:Fe = 4:1

For the catalyst characterization, X-Ray Diffraction (XRD), Scanning Electron Microscopy (SEM) and Brunauer-Emmet-Teller (BET) method have been used. All the samples of catalyst managed to undergo XRD characterization. Due to the technical problem, only four samples of catalyst has been tested using SEM method, which are:

1. Fe/ Al<sub>2</sub>O<sub>3</sub>
2. Co-Fe/ Al<sub>2</sub>O<sub>3</sub> – 1<sup>st</sup> sequence
3. Fe-Co/ Al<sub>2</sub>O<sub>3</sub> – 2<sup>nd</sup> sequence
4. Co-Fe/ Al<sub>2</sub>O<sub>3</sub> – co-impregnation

List of catalyst that undergo BET measurement are as follows:

1. Al<sub>2</sub>O<sub>3</sub>
2. Co/ Al<sub>2</sub>O<sub>3</sub>
3. Fe/ Al<sub>2</sub>O<sub>3</sub>
4. Co-Fe/ Al<sub>2</sub>O<sub>3</sub> – 1<sup>st</sup> sequence
5. Fe-Co/ Al<sub>2</sub>O<sub>3</sub> – 2<sup>nd</sup> sequence
6. Co-Fe/ Al<sub>2</sub>O<sub>3</sub> – co-impregnation

#### **4.1 Data Gathering and Analysis of Experimental Work**

##### **4.1.1 XRD Result:**

Basically, XRD is a basic tool for the determination of the atomic structure of solid phases in heterogeneous catalysis. Not only the identification of the bulk solid phases present in the catalyst, XRD also to determine the short range local order of the surface atoms which constitute the catalytic sites. Besides to identify the intensity peak, XRD is mainly to observe the crystalline phase of the samples. Following are the XRD result for all the samples of catalyst:

Figure 11: XRD Pattern for  $Al_2O_3$

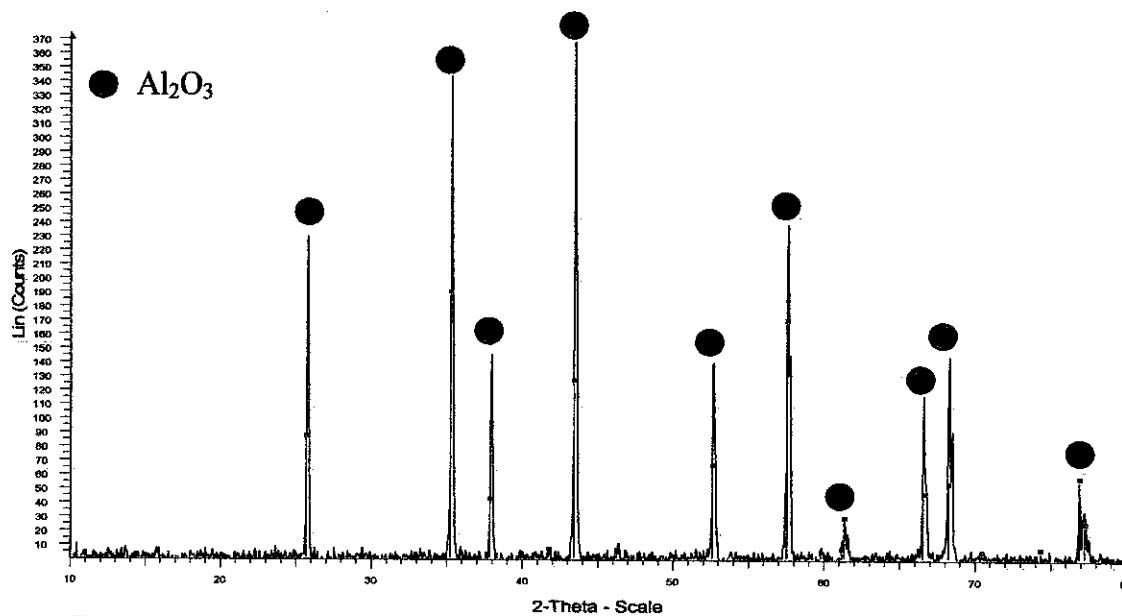


Figure 12: XRD Pattern for  $Fe/Al_2O_3$  and  $Co-Fe/Al_2O_3$

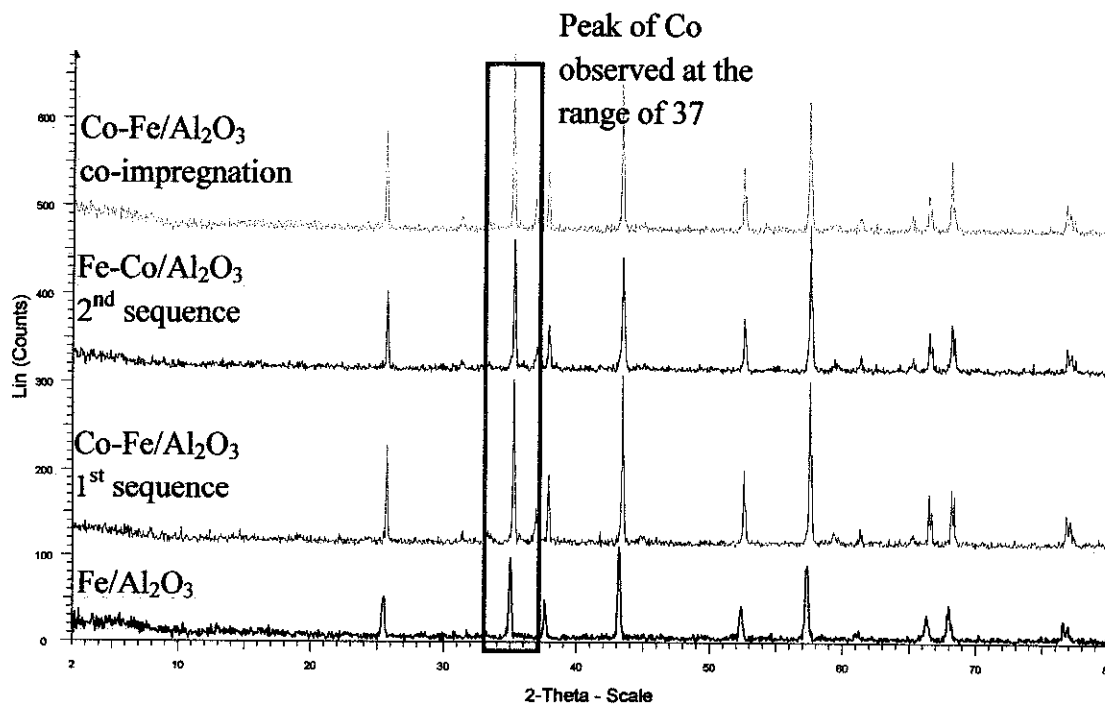
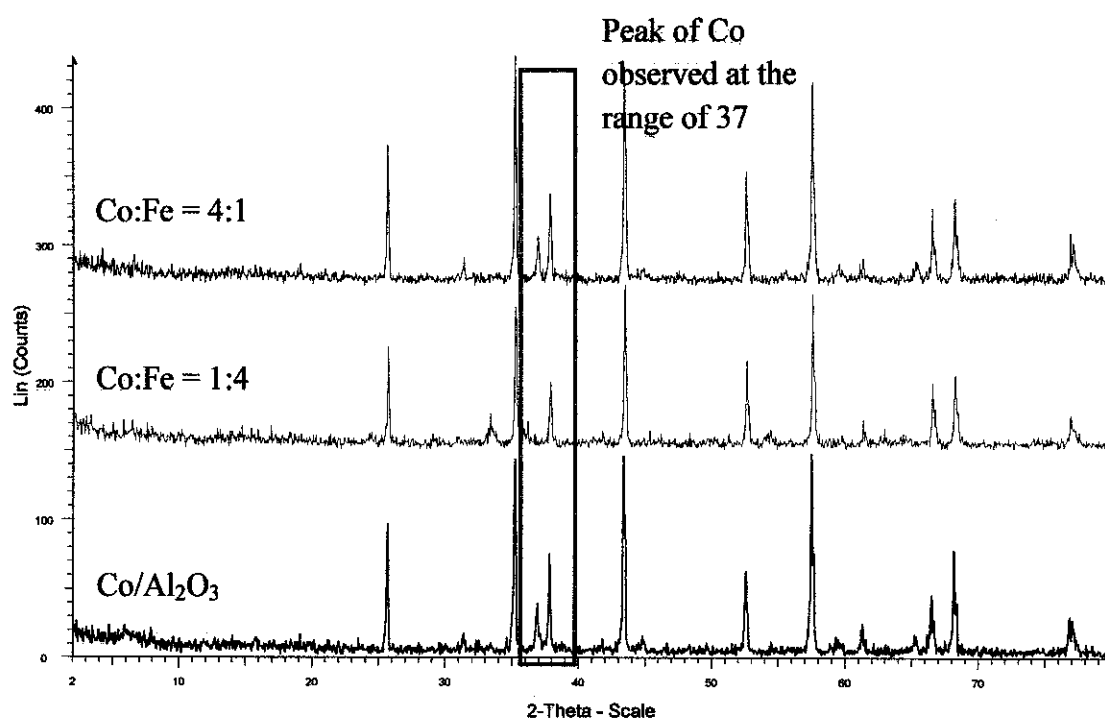


Figure 13: XRD Pattern for Co/Al<sub>2</sub>O<sub>3</sub>, Ratio Co:Fe=1:4 and Ratio Co:Fe=4:1



#### 4.1.2 SEM Result:

Basically, SEM is a type of electron microscope that images the sample surface by scanning it with a high-energy beam of electrons in a raster scan pattern. High magnification images provide the better view of particles distribution and manage to measure the size of nanoparticles. Following are the SEM result for four samples of catalyst from first batch:

Figure 14: SEM Photograph for Fe/Al<sub>2</sub>O<sub>3</sub>



Figure 15: SEM Photograph for Co-Fe/Al<sub>2</sub>O<sub>3</sub> (sequential)

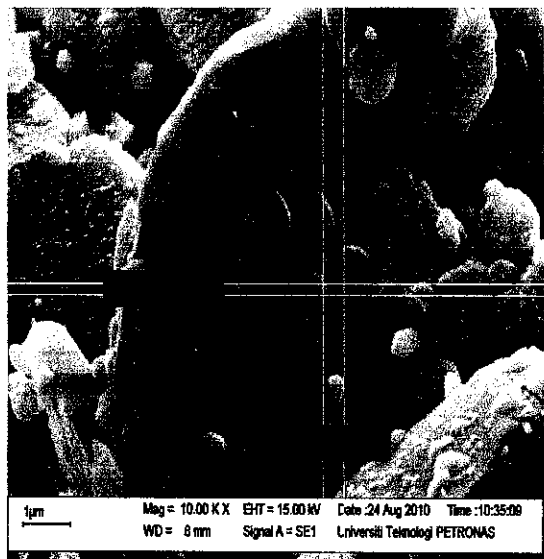


Figure 16: SEM Photograph for Fe-Co/Al<sub>2</sub>O<sub>3</sub> (sequential)

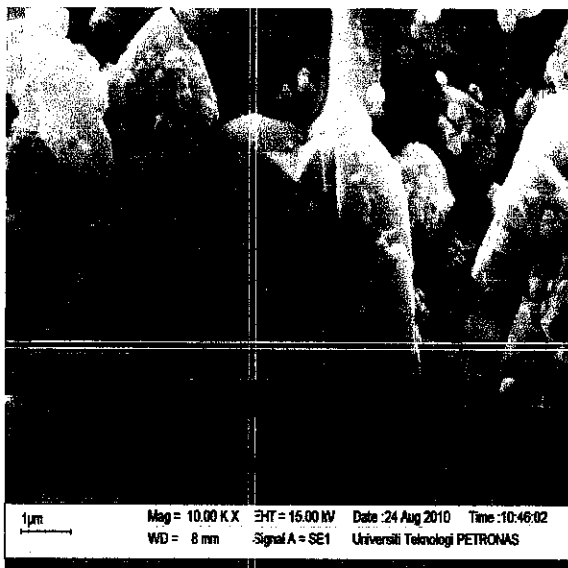
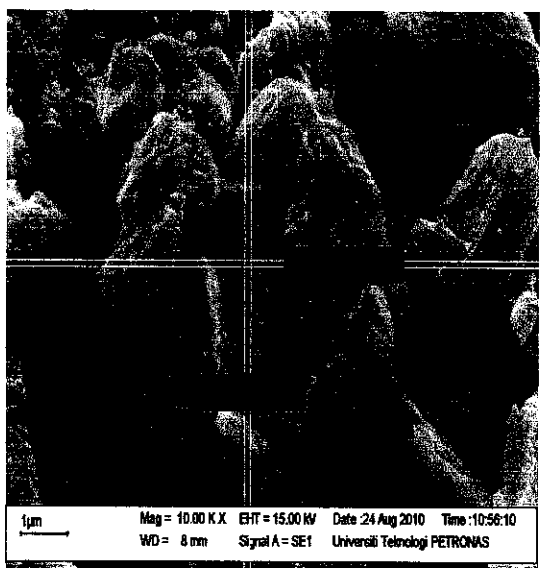


Figure 17: SEM Photograph for Co-Fe /Al<sub>2</sub>O<sub>3</sub> (co-impregnation method)





### 4.1.3 BET Result:

Table 4: Surface Area, Pore Volume and Pore Size for Al<sub>2</sub>O<sub>3</sub>

Surface Area, Pore Volume, Pore Size	Al <sub>2</sub> O <sub>3</sub>
<b>Surface Area:</b>	
<b>BJH Adsorption cumulative surface area of pores between 17.000 Å and 3000.000 Å width: (m<sup>2</sup>/g)</b>	<b>0.052</b>
<b>Pore Volume:</b>	
1) Single point adsorption total pore volume of pores less than 1273.117 Å width at P/Po = 0.984557724: (cm <sup>3</sup> /g)	0.000625
2) Single point desorption total pore volume of pores less than 700.728 Å width at P/Po = 0.971589758: (cm <sup>3</sup> /g)	0.000219
<b>3) BJH Adsorption cumulative volume of pores between 17.000 Å and 3000.000 Å width: (cm<sup>3</sup>/g)</b>	<b>0.001160</b>
<b>Pore Size:</b>	
<b>BJH Adsorption average pore width (4V/A): (Å)</b>	<b>890.054</b>

Table 5: Surface Area for Co/Al<sub>2</sub>O<sub>3</sub>, Fe/Al<sub>2</sub>O<sub>3</sub> and Co-Fe/Al<sub>2</sub>O<sub>3</sub>

Surface Area	Co/Al <sub>2</sub> O <sub>3</sub>	Fe/Al <sub>2</sub> O <sub>3</sub>	Co-Fe/ Al <sub>2</sub> O <sub>3</sub> (1 <sup>st</sup> sequence)	Fe-Co/ Al <sub>2</sub> O <sub>3</sub> (2 <sup>nd</sup> sequence)	Co-Fe/ Al <sub>2</sub> O <sub>3</sub> (co- impregnation)
1) Single point surface area at P/Po : (m <sup>2</sup> /g)	2.1373	2.6800	1.7704	1.3979	1.7798
2) BET Surface Area: (m <sup>2</sup> /g)	2.4213	3.0733	2.0300	1.7053	1.9672
3) Langmuir Surface Area: (m <sup>2</sup> /g)	3.8889	5.0062	3.2430	2.9340	3.0984
4) t-Plot External Surface Area: (m <sup>2</sup> /g)	3.2120	4.2231	2.6204	2.6025	2.4939
<b>5) BJH Adsorption cumulative surface area of pores between 17.000 Å and 3000.000 Å width: (m<sup>2</sup>/g)</b>	<b>1.709</b>	<b>3.068</b>	<b>1.413</b>	<b>1.431</b>	<b>1.929</b>
6) BJH Desorption cumulative surface area of pores between 17.000 Å and 3000.000 Å width: (m <sup>2</sup> /g)	1.4741	3.0981	1.1467	0.8853	2.1575

Table 6: Pore Volume for Co/Al<sub>2</sub>O<sub>3</sub>, Fe/Al<sub>2</sub>O<sub>3</sub> and Co-Fe/Al<sub>2</sub>O<sub>3</sub>

Pore Volume	Co/Al <sub>2</sub> O <sub>3</sub>	Fe/Al <sub>2</sub> O <sub>3</sub>	Co-Fe/ Al <sub>2</sub> O <sub>3</sub> (1 <sup>st</sup> sequence)	Fe-Co/ Al <sub>2</sub> O <sub>3</sub> (2 <sup>nd</sup> sequence)	Co-Fe/ Al <sub>2</sub> O <sub>3</sub> (co- impregnation)
1) Single point adsorption total pore volume of pores less than 1300 Å width at P/Po : (cm <sup>3</sup> /g)	0.004236	0.006802	0.005675	0.004131	0.008332
2) Single point desorption total pore volume of pores less than 750 Å width at P/Po: (cm <sup>3</sup> /g)	0.003460	0.006184	0.004780	0.003675	0.007723
3) t-Plot micropore volume: (cm <sup>3</sup> /g)	-0.000470	-0.000684	-0.000352	-0.000532	-0.000315
4) <b>BJH Adsorption cumulative volume of pores between 17.000 Å and 3000.000 Å width: (cm<sup>3</sup>/g)</b>	<b>0.005092</b>	<b>0.007873</b>	<b>0.006921</b>	<b>0.005153</b>	<b>0.010069</b>
5) BJH Desorption cumulative volume of pores between 17.000 Å and 3000.000 Å width: (cm <sup>3</sup> /g)	0.005009	0.007789	0.007002	0.004961	0.010030

Table 7: Pore Size for Co/Al<sub>2</sub>O<sub>3</sub>, Fe/Al<sub>2</sub>O<sub>3</sub> and Co-Fe/Al<sub>2</sub>O<sub>3</sub>

Pore Size	Co/Al <sub>2</sub> O <sub>3</sub>	Fe/Al <sub>2</sub> O <sub>3</sub>	Co-Fe/ Al <sub>2</sub> O <sub>3</sub> (1 <sup>st</sup> sequence)	Fe-Co/ Al <sub>2</sub> O <sub>3</sub> (2 <sup>nd</sup> sequence)	Co-Fe/ Al <sub>2</sub> O <sub>3</sub> (co- impregnation)
1) Adsorption average pore width (4V/A by BET): (Å)	69.9775	88.5281	111.8324	96.9023	169.4105
2) Desorption average pore width (4V/A by BET): (Å)	57.1597	80.4929	94.1783	86.1922	157.0285
3) <b>BJH Adsorption average pore width (4V/A): (Å)</b>	<b>119.149</b>	<b>102.644</b>	<b>195.959</b>	<b>144.030</b>	<b>208.836</b>
4) BJH Desorption average pore width (4V/A): (Å)	135.921	100.563	244.233	224.147	185.958

Figure 18: Isotherm Linear Plot for  $Al_2O_3$

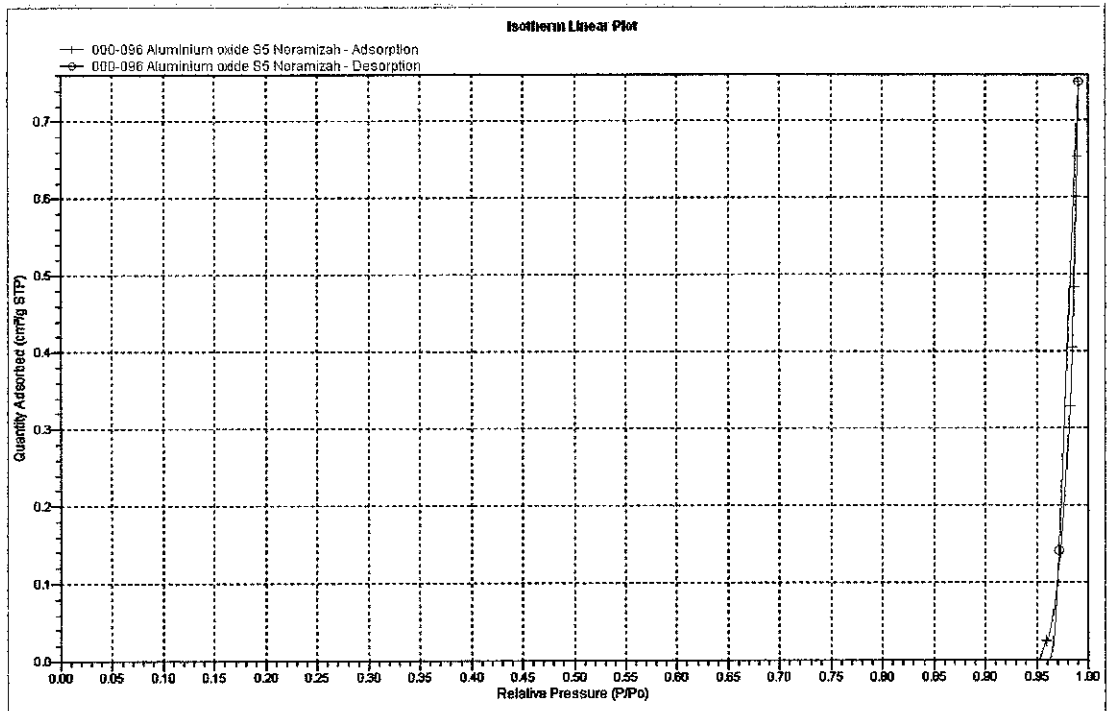


Figure 19: Isotherm Linear Plot for  $Co/Al_2O_3$

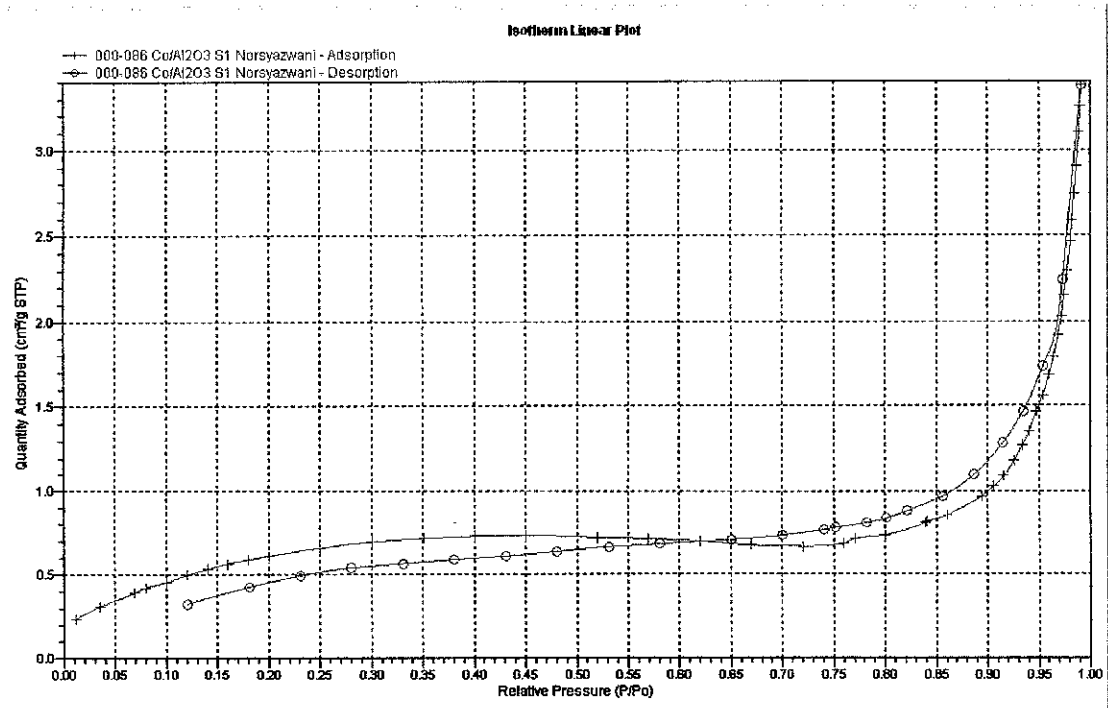


Figure 20: Isotherm Linear Plot for Fe/Al<sub>2</sub>O<sub>3</sub>

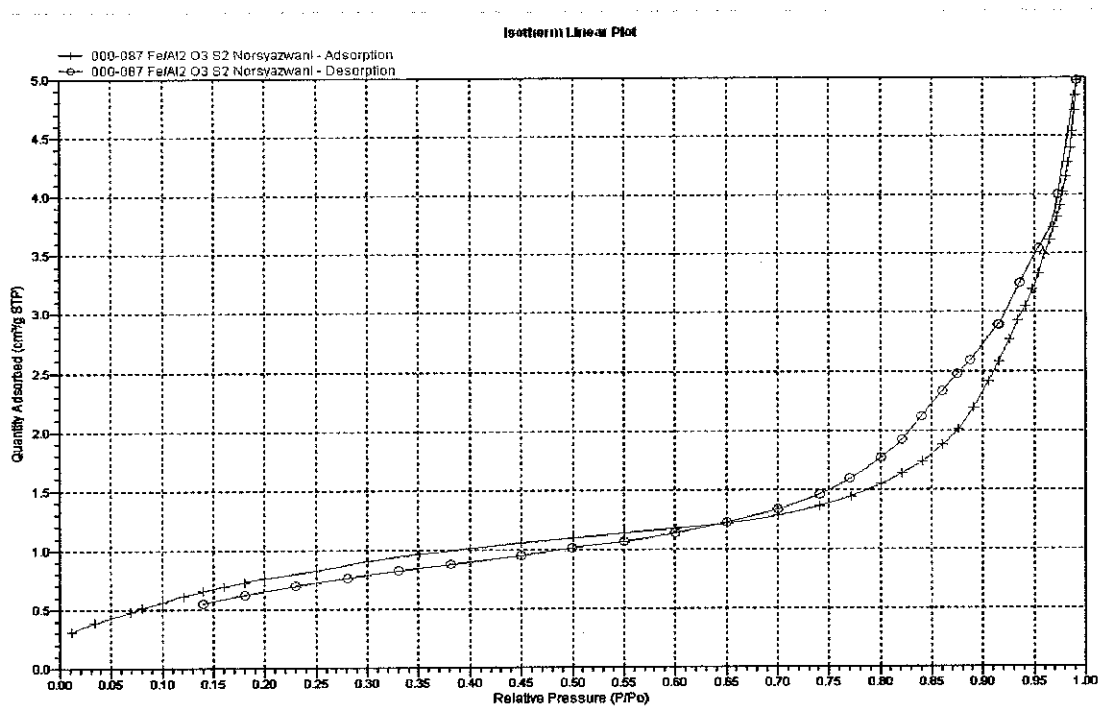


Figure 21: Isotherm Linear Plot for Co-Fe/Al<sub>2</sub>O<sub>3</sub> (sequential)

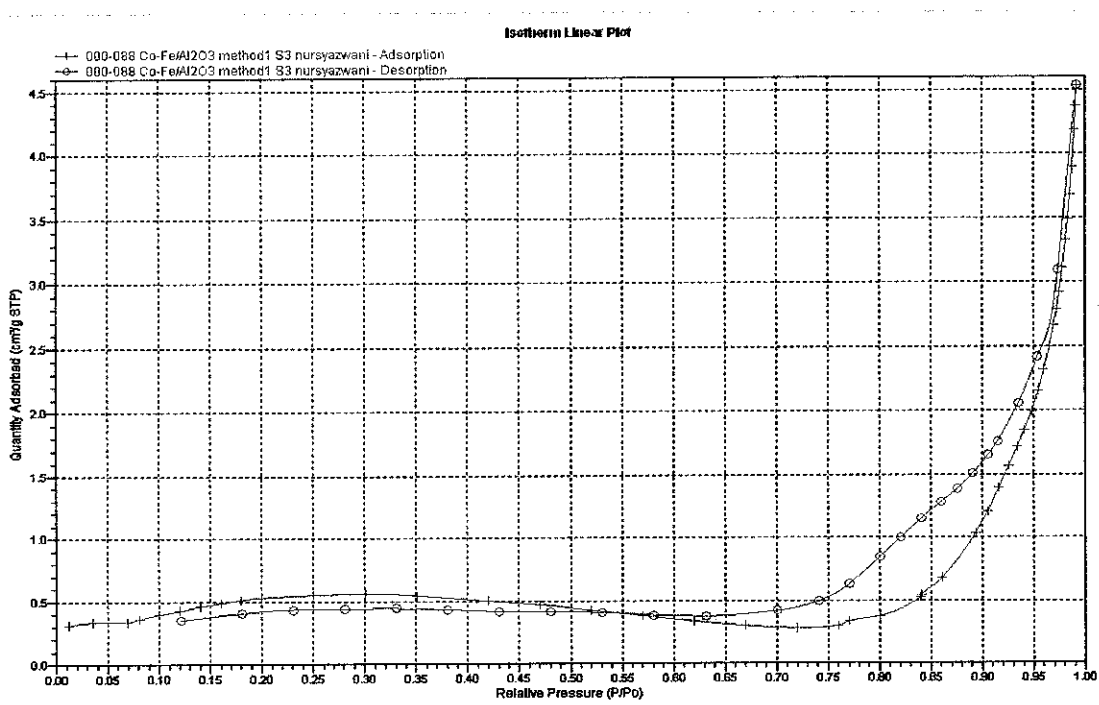


Figure 22: Isotherm Linear Plot for Fe-Co/Al<sub>2</sub>O<sub>3</sub> (sequential)

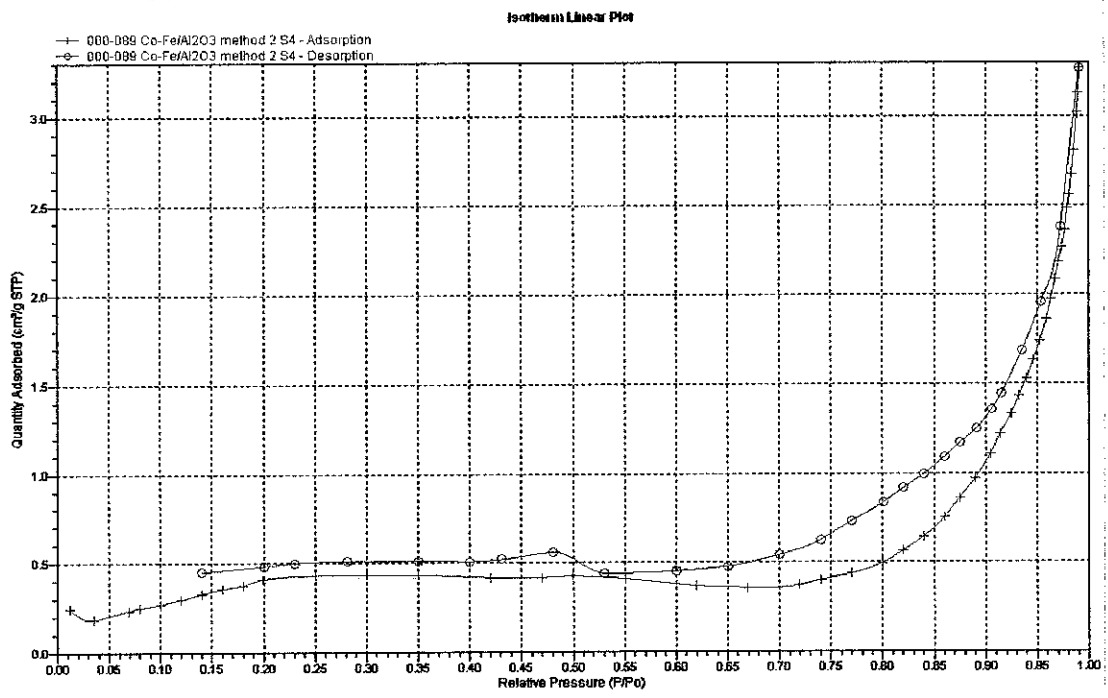
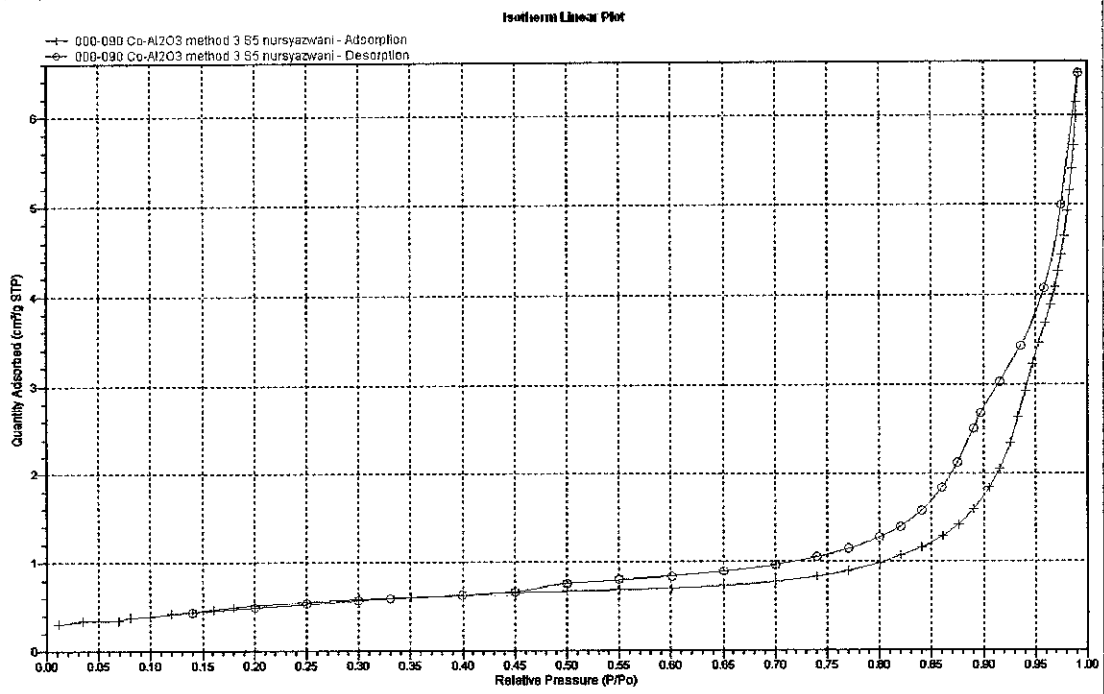


Figure 23: Isotherm Linear Plot for Fe-Co/Al<sub>2</sub>O<sub>3</sub> (co-impregnation)



## 4.2 Discussion on the Obtained Result

The main peak and reduction features observed from the result above indicate the presence of the Co/Fe species with different degrees of interaction with the support. From Figure 12, it can be concluded that there are another peak appeared in the sample from sample Fe/Al<sub>2</sub>O<sub>3</sub> and Co-Fe/ Al<sub>2</sub>O<sub>3</sub> (1<sup>st</sup>, 2<sup>nd</sup> sequence and co-impregnation) as the addition of Cobalt into the solution. The additional peak was observed at the range of 37. The intensity of the peak is increased for the sample that contained Cobalt when compared to the sample of Fe/Al<sub>2</sub>O<sub>3</sub> alone. The same result observed on Figure 13 where the intensity of the peak increased when the ratio of Cobalt increased. This is because the Cobalt and Al<sub>2</sub>O<sub>3</sub> peak overlapped thus affect the intensity of the Al<sub>2</sub>O<sub>3</sub>. Besides, the Cobalt particles competed with Iron particles to fill up the pores on the supported catalyst. This will contribute to the lack of the uniformity in the stacking pattern of the layers. There is no peak for Iron observed on the samples as it is highly dispersed form.

All the peaks observed from Figure 12 and Figure 13 is in agreement with the peak observed on Figure 11. Each peak appeared at the same range, thus all the peaks was detected as alumina. Based on Figure 26 (see appendices), when the XRD pattern for Al<sub>2</sub>O<sub>3</sub> was compared, it can be concluded that the supported catalyst used in this project was  $\alpha$ -Al<sub>2</sub>O<sub>3</sub>. High intensity of the peak of  $\alpha$ -Al<sub>2</sub>O<sub>3</sub> is observed based on Figure 11. Basically, XRD pattern for  $\gamma$ - Al<sub>2</sub>O<sub>3</sub> is decreasing and formed broadening peak instead of sharp peak as presented by  $\alpha$ -Al<sub>2</sub>O<sub>3</sub>. Thus, in order to determine the peak behavior of  $\alpha$ -Al<sub>2</sub>O<sub>3</sub>, XRD characterization was carried out on support catalyst independently. This can be referred to Figure 11. The sharp peaks originating from metal aluminates were visible in the XRD patterns of the samples, usually no spinel diffraction peaks could be discerned for  $\gamma$ - Al<sub>2</sub>O<sub>3</sub> samples. This means that no large Co or Fe /Al<sub>2</sub>O<sub>3</sub> particles were formed on the  $\gamma$ - Al<sub>2</sub>O<sub>3</sub> slices, in contrast to the  $\alpha$ -Al<sub>2</sub>O<sub>3</sub> substrate. Apparently, the spinel particles are too small to give rise to diffraction peaks that are discernible from the broad  $\gamma$ - Al<sub>2</sub>O<sub>3</sub> peaks, or the solid- state reaction is confined to the few monolayers of each  $\gamma$ - Al<sub>2</sub>O<sub>3</sub> grain in the surface region of the substrates.

For steam reforming process,  $\gamma$ - $\text{Al}_2\text{O}_3$  was determined to be the most preferred support coating, stabilized and higher surface area transition. The high grain boundary density of  $\gamma$ - $\text{Al}_2\text{O}_3$  is a major reason for its high reactivity toward aluminate formation, as compared to  $\alpha$ - $\text{Al}_2\text{O}_3$ . The “defect spinel structure” of  $\gamma$ - $\text{Al}_2\text{O}_3$  may also have a beneficial effect on the solid-state reaction between transition metal oxides and  $\gamma$ - $\text{Al}_2\text{O}_3$ ; it will facilitate cations to enter the alumina lattice. Because of these solid-state transformations, an enhanced reactivity of the alumina is also expected. Even though  $\alpha$ - $\text{Al}_2\text{O}_3$  has lower surface area, the rate of activity is higher and gives high conversion at higher temperature such as at  $800^\circ\text{C}$ . This reaction is observed for methane oxidation over Pd-catalyst supported on  $\alpha$ - $\text{Al}_2\text{O}_3$ .

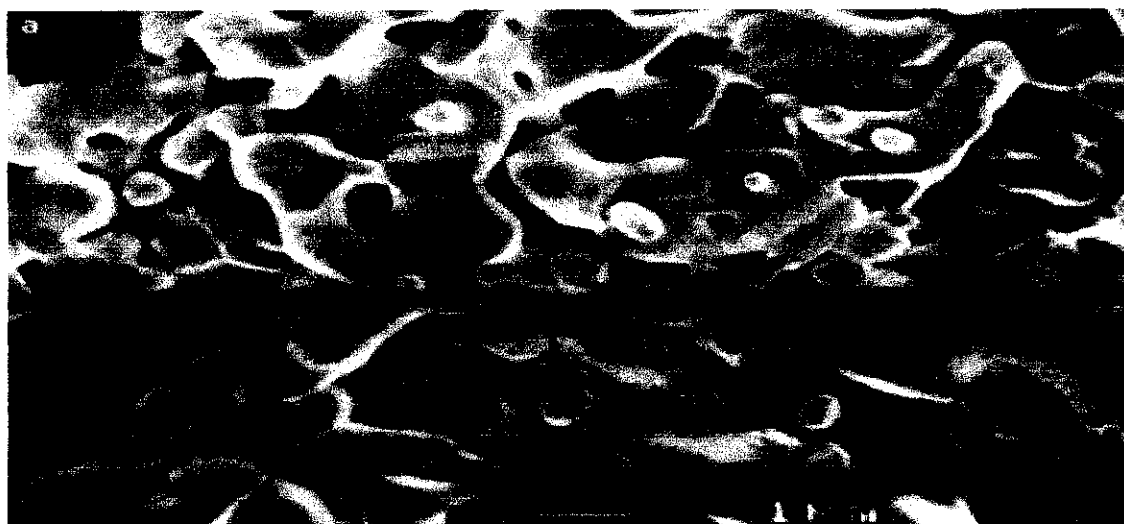
When the ratio of precursors is varied, the XRD pattern for the samples can be observed on Figure 13. The peak that observed at the range of 37 is definitely goes to Cobalt. This is because, when the ratio of Cobalt is lower than Iron, there is no peak appeared at the range of 37 on Figure 18. Even though the ratio of Iron is high, there is no peak observed for Iron. The above statement supported that as the amount of Cobalt in the form of Cobalt Oxide increases, the average size of Iron particles being in metal form and becomes smaller. This can be concluded that, Iron is highly dispersed for all the samples.

In 1 atm high-purity  $\text{N}_2$ ,  $\text{Fe}_3\text{O}_4$  (magnetite) is the stable iron oxide. It reacts with  $\text{Al}_2\text{O}_3$  to a mixed hercynite-magnetite compound ( $\text{FeAl}_2\text{O}_4 \cdot x\text{Fe}_3\text{O}_4$ ); the minimum value of  $x$  depends critically on the oxygen partial pressure. The reaction rate of  $\text{CoO}_x$  and  $\text{FeO}_x$  with alumina to  $\text{CoAl}_2\text{O}_4$  and  $\text{FeAl}_2\text{O}_4$  was found to follow the sequence  $\text{FeAl}_2\text{O}_4 < \text{CoAl}_2\text{O}_4$  [10]. The low reactivity of iron oxides with alumina in either 1 atm  $\text{O}_2$  or  $\text{N}_2$  is explained by thermodynamic considerations.  $\text{Fe}_2\text{O}_3$  (hematite) is the thermodynamically stable iron oxide at  $1000^\circ\text{C}$  in 1 atm  $\text{O}_2$ , which can dissolve some  $\text{Al}_2\text{O}_3$  but does not react to  $\text{FeAl}_2\text{O}_4$  (hercynite). Thus, it can be concluded that the relative stability of  $\text{Fe}^{3+}$  with respect to  $\text{Fe}^{2+}$  protects  $\text{FeO}_x/\text{Al}_2\text{O}_3$  model systems from  $\text{FeAl}_2\text{O}_4$  formation. The stability of metal oxidation states higher than +2 suppresses spinel formation in several other metal with  $\text{Al}_2\text{O}_3$  systems.

From the SEM result obtained, it can be seen that both metal, Cobalt and Iron were coated on the  $\text{Al}_2\text{O}_3$  surface. When compared figure 21 with figure 22, 23 and 24, more nanoparticles coated on the supported catalyst as the addition of both metal into the samples. This indicates higher concentrations of metal precursors and its compound. Some small (100-200 nm) nearly spherical particles are apparent which may be comprised of the Co and Fe binder material or  $\text{Al}_4\text{C}_3$  formed from burnout material used to control pore size during support preparation. The bigger particles indicate for  $\text{Al}_2\text{O}_3$  supported catalyst, and there is a change in the morphology between the support and the precursors. In agreements with the XRD pattern, as the entire main peak observed detected as  $\text{Al}_2\text{O}_3$ , considerably larger particles are present for the  $\text{Al}_2\text{O}_3$ . As both metals dissolved into the solution, it is found that the nanoparticles evenly distributed which is had smaller visible patches/ particles that were more scattered when compared to the single metal catalyst. Pore structures were found to greatly influence the size, shape and appearance of the pellets in the sample prepared. The bare  $\alpha\text{-Al}_2\text{O}_3$  appears to be rather structureless, but it is actually crystalline with a very flat planar surface exposed. Careful inspection reveals information about the crystalline structure and the presence of terraced layers leading up to the exposed plane. The micrograph taken from the catalyst shows that the alumina support appears to be quite uniformly coated with Co and Fe. The planar  $\alpha\text{-Al}_2\text{O}_3$  structure can be observed at some points in the micrograph. The assertion that the coating is quite uniform is consistent with the XRD data that were taken from both the support and the catalyst at two different points on each sample. The points were selected to give a maximum compositional difference based on differences in appearance in the SEM micrographs. Same behavior of  $\alpha\text{-Al}_2\text{O}_3$  presented in the recent study as shown in the Figure 18. The  $\alpha\text{-Al}_2\text{O}_3$  has a crystalline structure with a well-defined flat surface plane exposed.



Figure 24: SEM Photograph for  $\alpha$ - $\text{Al}_2\text{O}_3$  [11]



Surface area of catalysts is the most important in adsorption measurements. The rate of transport of reactants to the surface, and of products away from the surface is proportional to the surface area of the active phase of the catalyst when the observed rate is faster than the catalysed reaction. It is normally desirable for the catalyst to have a high surface area, but there is a limit to what can be achieved merely by making the particle size very small. Based on the BET result obtained, the BJH Adsorption cumulative surface area of pores between 17.000 Å and 3000.000 Å width for Ferum is higher than Cobalt which is 3.069  $\text{m}^2/\text{g}$  and 1.709  $\text{m}^2/\text{g}$  respectively. Compared to the bi-metallic catalyst, the average surface area is  $\sim 1\text{-}2$   $\text{m}^2/\text{g}$ . Surface area is decreasing when both Cobalt and Ferum are dissolved into the sample. Smaller surface area of  $\text{Al}_2\text{O}_3$  which is 0.052  $\text{m}^2/\text{g}$  is in agreement that the support used is  $\alpha$ -  $\text{Al}_2\text{O}_3$ .

From previous study, the calcined catalyst has lower BET surface area ( $S_{\text{BET}}$ ) than the supports and they show decreasing BET surface area with increasing Co loading as shown in the table below. These changes are suspected to be caused by plugging of support pores due to agglomeration of cobalt oxide [12].

Table 8: BET Surface Area with Different Co Loading

SAMPLE	SURFACE AREA (m <sup>2</sup> /g)	VOL. PORE (cc/g)	DIAM. PORE (Å)	ISOTHERM TYPE	PORE TYPE
M-6 1%Co	676	1.34	74	IV	MESOPORES
M-6 3%Co	660	1.28	74	IV	MESOPORES
M-6 5%Co	617	1.23	75	IV	MESOPORES

In addition to knowing the total surface area, including that provided by the pores, it is useful also to measure the volume of the pores and their average size and size distribution is also of interest. For the pore volume measurement, the BJH Adsorption cumulative volume of pores between 17.000 Å and 3000.000 Å width for Al<sub>2</sub>O<sub>3</sub> is 0.001160 cm<sup>3</sup>/g. The value is smaller when compared to the both single and bi-metallic catalyst which is ~0.005-0.007 cm<sup>3</sup>/g. When compared between sequential and co-impregnation method, the co-impregnated catalyst shows highest value which is ~0.01 cm<sup>3</sup>/g. While for the pore size, the BJH Adsorption average pore width for Al<sub>2</sub>O<sub>3</sub> is 890.054 Å. This is a large value compared to the single and bi-metallic catalyst which is ~100-200 Å.

The surface area of a solid can be determined from the Langmuir adsorption isotherm. If the adsorption of a gas is measured at a temperature well above that at which it condenses to a liquid, so that a second layer does not build up over the first layer, then the maximum number of molecules adsorbed can be used to estimate the surface area. Referring to Figure 18-23, the Langmuir isotherm is the form of Type IV and hysteresis loop of Type B which is open slit- shaped capillaries. This is in agreement when referring to Figure 25 and Figure 26 where the isotherm does not follow the same path in desorption as it does in adsorption. The reason for this is that evaporation of condensed gas in fine pores does not occur as easily as its condensation. This is because a molecule evaporating from a highly curved meniscus has a higher probability of recondensing than one evaporating from a plane surface.

Figure 25: Classification of Isotherms According to the BET Theory

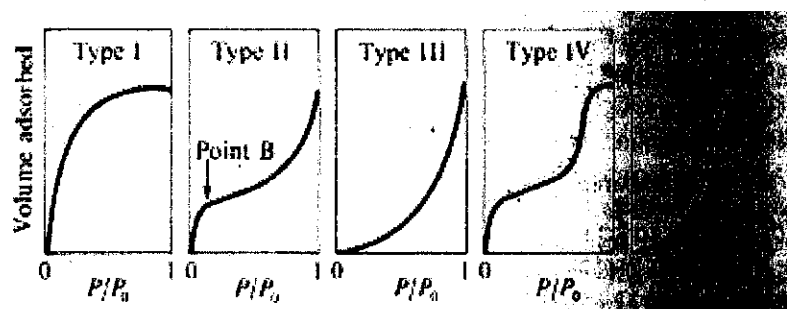
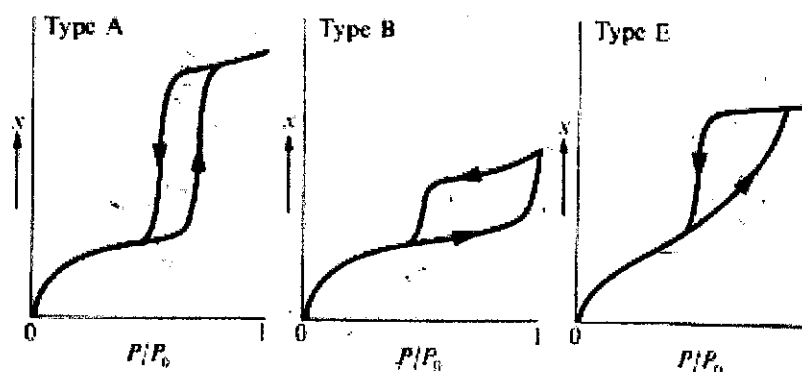


Figure 26: Hysteresis Loops on Type IV Isotherms



From all the results obtained, it can be concluded that the properties of Cobalt and Ferum are summarized below:

Table 9: Properties of Cobalt and Ferum

Cobalt	Ferum
1. Hard ferromagnetic, silver-white, hard, lustrous, brittle element	1. Lustrous, ductile, malleable, silver-gray metal
2. Can be magnetized	2. Rusts in dump air, but not in dry air
3. Active chemically, stable in air and unaffected by water	3. Chemically active and forms two major series of chemical compounds, Ferrous and Ferric

As one of the study conducted earlier, Co/Al<sub>2</sub>O<sub>3</sub> catalysts had shown average conversions, higher than 70% for the steam reforming of ethanol at 400°C. An increase of ethanol conversion and reduction of liquid products were observed on the catalysts with higher cobalt contents. Hydrogen is the main constituent of the reaction effluent, which also contains CO, CO<sub>2</sub> and CH<sub>4</sub>. Ethylene formation occurred only on the Co/Al<sub>2</sub>O<sub>3</sub> catalyst with small Co contents ( $\leq 8\%$ ). After ethanol reforming, the CO produced can react with water (WGS) or hydrogen (methanation) on Co sites. Both reactions show high conversion on Co/Al<sub>2</sub>O<sub>3</sub> and shows higher efficiency for CO removal.

Another study revealed that catalytic activity on Co catalyst modified with another metal which is Fe for steam reforming of ethanol show that Fe loading had a positive effect and it is thought that Fe addition promotes steam reforming of ethanol preferentially without promoting decomposition of CH<sub>3</sub>CHO from selectivity to products. The Fe modified Co catalyst showed a stable high activity and the highest selectivity to steam reforming, with low carbon deposits.

## CHAPTER 5

### CONCLUSION AND RECOMMENDATION

#### 5.1 Conclusion

The Co-Fe/Al<sub>2</sub>O<sub>3</sub> catalyst for steam reforming of ethanol was prepared using incipient wetness method with sequential and co-impregnation method. From experimental work, it can be concluded that the co-impregnation method takes less time compared to the sequential methods. The catalyst was characterized using XRD, SEM, BET and TPR/D. Based on the XRD, SEM and BET result obtained, the characteristic for both sequential and co-impregnated catalyst prepared present the similar result. This can be concluded that the sequence of the metal did not much influence on the crystalline phase, morphology and surface area of the catalyst. The combination of Cobalt and Ferum supported on Al<sub>2</sub>O<sub>3</sub> gives high stabilizing oxide, longer lifetime and resulted as active metal.

#### 5.2 Recommendation

For the future work continuation, catalyst testing will be implemented to measure the hydrogen production, analyze the catalytic activity and etc. for steam reforming of ethanol. Further study need to be made on the particles image to identify the type and compositions of nanoparticles for each image captured. In order to obtain more significant result, the weight percentage of metal loading has to be increased especially on Ferum since it is highly dispersed on the sample. The support used for steam reforming process has to be set to  $\gamma$ -Al<sub>2</sub>O<sub>3</sub> as the most preferred support coating, stabilized, higher surface area transition and higher grain boundary density.

## REFERENCES

- [1] Llorca J, Homs N, Piscina PR., (2004). In situ DRIFT- mass spectrometry study of the ethanol steam-reforming reaction over carbonyl-derived Co/ZnO catalysts, *J Catal*, 227, pp 556–60.
- [2] Meng Ni, Dennis Y.C. Leung, Micheal K. H. Leung., (2007). A review on reforming bio- ethanol for hydrogen production, *International Journal of Hydrogen Energy*, 32, pp 3238-3247.
- [3] Marcelo S. Batista, Rudy K.S. Santos, Elisabete M. Assaf, Jose M. assaf, edson A. Ticianelli., (2004). High efficiency steam reforming of ethanol by cobalt-based catalyst, *J Power Sources*, 134, pp 27-32.
- [4] Vaidya PD, Rodrigues AE., (2006). Insights into steam reforming of ethanol to produce hydrogen for fuel cells, *Chem Eng*, 117, pp 39–49.
- [5] Batista MS, Santos RKS, Assaf EM, Assaf JM, Ticianelli EA., (2003). Characterization of the activity and stability of supported cobalt catalysts for the steam reforming of ethanol, *J Power Sources*, 124, pp 99-103.
- [6] Bunjerd Jongsomjit, Joongjai Panpranot and James G. Goodwin Jf., (2003). Effect of Zirconia- modified alumina on the properties of Co/  $\gamma$ -Al<sub>2</sub>O<sub>3</sub> catalysts, *Journal of Catalysis*, 215, pp 66-77.
- [7] Batista MS, Santos RKS, Assaf EM, Assaf JM, Ticianelli EA., (2004). High efficiency steam reforming of ethanol by cobalt- based catalysts, *J Power Sources*, 134, pp 27-32.
- [8] Yasushi Sekine, Atsushi Kazama, Yoshiyuki Izutsu, Masahiko Matsukata, Eiichi Kikuchi., (2009). Steam reforming of ethanol over cobalt catalyst modified with small amount of iron, *Catal Lett*, 132, pp 329-334.
- [9] Francesco Pinna., (1998). Supported metal catalysts preparation, *Catalysis Today*, 41, pp 129-137.

- [10] P.H. Bolt, F.H.P.M. Habraken and J.W. Geus., (1998). Formation of Nickel, Cobalt, Copper and Iron Aluminates from  $\alpha$ - and  $\gamma$ -Alumina-Supported Oxides: A Comparative Study, *Journal of solid state chemistry*, 135, pp 59-69.
- [11] Jens Sehested., (2006). Four challenges for nickel steam reforming catalysts, *Catalysis Today*, 111, pp 103-110.
- [12] A. Páramo Garcia, Esthela Ramos R., G. del Angel, J. Navarrete and Cesar A. Contreras., (2007). Catalytic Activity of Supported Cobalt Catalyst in the Crotonaldehyde Hydrogenation Reaction.
- [13] Wei- Ping Dow, Yu- Piao Wang, Ta- Jen Huang., (2000). TPR and XRD studies of yttria- doped ceria/  $\gamma$ - alumina- supported copper oxide catalyst, *Applied Catalysis A: General*, 190, pp 25-34.
- [14] P.H. Bolt, F.H.P.M. Habraken and J.W. Geus., (1998). Formation of Nickel, Cobalt, Copper and Iron Aluminates from  $\alpha$ - and  $\gamma$ -Alumina- supported oxides, *Journal of Solid State Chemistry*, 135, pp 59-69.

## APPENDICES

### Method 1: incipient wetness method (single metal)

Catalyst: Co/Al<sub>2</sub>O<sub>3</sub>



Find Mass: 50g

5% : 2.5g metal (Co)

95% : 47.5g support (Al<sub>2</sub>O<sub>3</sub>)

Calculation:

1) MW of Co(NO<sub>3</sub>)<sub>2</sub>·6(H<sub>2</sub>O) is 291.03 g/mol

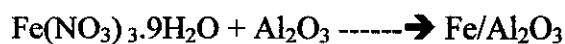
In 291.03 g/mol of Co(NO<sub>3</sub>)<sub>2</sub>·6(H<sub>2</sub>O), has 58.93 g/mol of Co.

In order to get **2.5g of Co** only, weight of **Co(NO<sub>3</sub>)<sub>2</sub>·6(H<sub>2</sub>O)** that will be used should be **12.3472 g**.

Thus, **12.3472 g of Co(NO<sub>3</sub>)<sub>2</sub>·6(H<sub>2</sub>O) + 47.5 g of Al<sub>2</sub>O<sub>3</sub>** to get 50 g of Co/Al<sub>2</sub>O<sub>3</sub>.  
**(2.5 g of Co)**

### Method 2: incipient wetness method (single metal)

Catalyst: Fe/Al<sub>2</sub>O<sub>3</sub>



Find Mass: 50g

5% : 2.5g metal (Fe)

95% : 47.5g support (Al<sub>2</sub>O<sub>3</sub>)



Calculation:

1) MW of  $\text{Fe}(\text{NO}_3)_3 \cdot 9\text{H}_2\text{O}$  is 404 g/mol

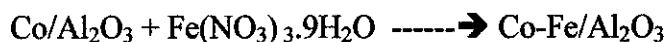
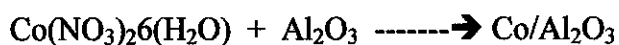
In 404 g/mol of  $\text{Fe}(\text{NO}_3)_3 \cdot 9\text{H}_2\text{O}$ , has 55.845 g/mol of Fe.

In order to get **2.5g of Fe** only, weight of  $\text{Fe}(\text{NO}_3)_3 \cdot 9\text{H}_2\text{O}$  that will be used should be **18.0858 g**.

Thus, **18.0858 g of  $\text{Fe}(\text{NO}_3)_3 \cdot 9\text{H}_2\text{O}$  + 47.5 g of  $\text{Al}_2\text{O}_3$**  to get 50 g of Fe/ $\text{Al}_2\text{O}_3$ .  
(2.5 g of Fe)

**Method 3: incipient wetness method (bi-metal)**

Catalyst: Co-Fe/ $\text{Al}_2\text{O}_3$



Find Mass: 50g

5% : 2.5g metal each (Co and Fe)

95% : 47.5g support ( $\text{Al}_2\text{O}_3$ )

Calculation:

1) MW of  $\text{Co}(\text{NO}_3)_2 \cdot 6\text{H}_2\text{O}$  is 291.03 g/mol

In 291.03 g/mol of  $\text{Co}(\text{NO}_3)_2 \cdot 6\text{H}_2\text{O}$ , has 58.93 g/mol of Co.

In order to get **2.5g of Co** only, weight of  $\text{Co}(\text{NO}_3)_2 \cdot 6\text{H}_2\text{O}$  that will be used should be **12.3472 g**.

Thus, **12.3472 g of  $\text{Co}(\text{NO}_3)_2 \cdot 6\text{H}_2\text{O}$  + 47.5 g of  $\text{Al}_2\text{O}_3$**  to get 50 g of Co/ $\text{Al}_2\text{O}_3$ .  
(2.5 g of Co)

2) MW of  $\text{Fe}(\text{NO}_3)_3 \cdot 9\text{H}_2\text{O}$  is 404 g/mol

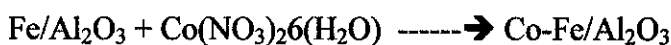
In 404 g/mol of  $\text{Fe}(\text{NO}_3)_3 \cdot 9\text{H}_2\text{O}$ , has 55.845 g/mol of Fe.

In order to get **2.5g of Fe** only, weight of  $\text{Fe}(\text{NO}_3)_3 \cdot 9\text{H}_2\text{O}$  that will be used should be **18.0858 g**.

Thus, **18.0858 g of  $\text{Fe}(\text{NO}_3)_3 \cdot 9\text{H}_2\text{O}$  + 47.5 g of  $\text{Co}/\text{Al}_2\text{O}_3$**  to get 50 g of  $\text{Co-Fe}/\text{Al}_2\text{O}_3$ .  
**(2.5 g of Fe)**

#### **Method 4: incipient wetness method (bi-metal)**

Catalyst:  $\text{Fe-Co}/\text{Al}_2\text{O}_3$



Find Mass: 50g

5% : 2.5g metal each (Co and Fe)

95% : 47.5g support ( $\text{Al}_2\text{O}_3$ )

Calculation:

1) MW of  $\text{Fe}(\text{NO}_3)_3 \cdot 9\text{H}_2\text{O}$  is 404 g/mol

In 404 g/mol of  $\text{Fe}(\text{NO}_3)_3 \cdot 9\text{H}_2\text{O}$ , has 55.845 g/mol of Fe.

In order to get **2.5g of Fe** only, weight of  $\text{Fe}(\text{NO}_3)_3 \cdot 9\text{H}_2\text{O}$  that will be used should be **18.0858 g**.

Thus, **18.0858 g of  $\text{Fe}(\text{NO}_3)_3 \cdot 9\text{H}_2\text{O}$  + 47.5 g of  $\text{Al}_2\text{O}_3$**  to get 50 g of  $\text{Fe}/\text{Al}_2\text{O}_3$ .  
**(2.5 g of Fe)**

2) MW of  $\text{Co}(\text{NO}_3)_2 \cdot 6\text{H}_2\text{O}$  is 291.03 g/mol

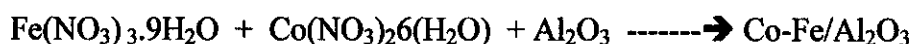
In 291.03 g/mol of  $\text{Co}(\text{NO}_3)_2 \cdot 6\text{H}_2\text{O}$ , has 58.93 g/mol of Co.

In order to get **2.5g of Co** only, weight of  $\text{Co}(\text{NO}_3)_2 \cdot 6\text{H}_2\text{O}$  that will be used should be **12.3472 g**.

Thus, **12.3472 g of  $\text{Co}(\text{NO}_3)_2 \cdot 6\text{H}_2\text{O}$  + 47.5 g of  $\text{Fe}/\text{Al}_2\text{O}_3$**  to get 50 g of Co-Fe/ $\text{Al}_2\text{O}_3$ .  
**(2.5 g of Co)**

### **Method 5: co-impregnation method**

Catalyst: Co-Fe/ $\text{Al}_2\text{O}_3$



Find Mass: 50g

2.5% : 2.5g metal (Co)

2.5% : 2.5g metal (Fe)

95% : 45g support ( $\text{Al}_2\text{O}_3$ )

Calculation:

MW of  $\text{Co}(\text{NO}_3)_2 \cdot 6\text{H}_2\text{O}$  is 291.03 g/mol

In 291.03 g/mol of  $\text{Co}(\text{NO}_3)_2 \cdot 6\text{H}_2\text{O}$ , has 58.93 g/mol of Co.

In order to get **2.5g of Co** only, weight of  $\text{Co}(\text{NO}_3)_2 \cdot 6\text{H}_2\text{O}$  that will be used should be **12.3472 g**.

MW of  $\text{Fe}(\text{NO}_3)_3 \cdot 9\text{H}_2\text{O}$  is 404 g/mol

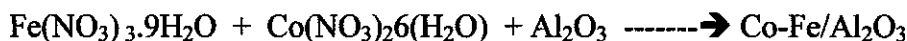
In 404 g/mol of  $\text{Fe}(\text{NO}_3)_3 \cdot 9\text{H}_2\text{O}$ , has 55.845 g/mol of Fe.

In order to get **2.5g of Fe** only, weight of  $\text{Fe}(\text{NO}_3)_3 \cdot 9\text{H}_2\text{O}$  that will be used should be **18.0858 g**.

Thus, **12.3472 g of  $\text{Co}(\text{NO}_3)_2 \cdot 6\text{H}_2\text{O}$**  + **18.0858 g of  $\text{Fe}(\text{NO}_3)_3 \cdot 9\text{H}_2\text{O}$**  + **45 g of  $\text{Al}_2\text{O}_3$**   
to get 50 g of Co-Fe/ $\text{Al}_2\text{O}_3$ .  
(2.5 g of Co) (2.5 g of Fe)

**Method 6: co-impregnation method**

Catalyst: Co-Fe/ $\text{Al}_2\text{O}_3$



Find Mass: 50g

2.5% : 2.5g metal (Co)

2.5% : 2.5g metal (Fe)

95% : 45g support ( $\text{Al}_2\text{O}_3$ )

Ratio  $\rightarrow$  Co:Fe = 1:4

Calculation:

MW of  $\text{Co}(\text{NO}_3)_2 \cdot 6\text{H}_2\text{O}$  is 291.03 g/mol

In 291.03 g/mol of  $\text{Co}(\text{NO}_3)_2 \cdot 6\text{H}_2\text{O}$ , has 58.93 g/mol of Co.

In order to get **1g of Co** only, weight of  **$\text{Co}(\text{NO}_3)_2 \cdot 6\text{H}_2\text{O}$**  that will be used should be **4.9386 g**.

MW of  $\text{Fe}(\text{NO}_3)_3 \cdot 9\text{H}_2\text{O}$  is 404 g/mol

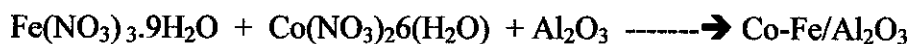
In 404 g/mol of  $\text{Fe}(\text{NO}_3)_3 \cdot 9\text{H}_2\text{O}$ , has 55.845 g/mol of Fe.

In order to get **4g of Fe** only, weight of  **$\text{Fe}(\text{NO}_3)_3 \cdot 9\text{H}_2\text{O}$**  that will be used should be **28.8571 g**.

Thus, **4.9386 g of  $\text{Co}(\text{NO}_3)_2 \cdot 6\text{H}_2\text{O}$**  + **28.8571 g of  $\text{Fe}(\text{NO}_3)_3 \cdot 9\text{H}_2\text{O}$**  + **45 g of  $\text{Al}_2\text{O}_3$**  to  
get 50 g of Co-Fe/ $\text{Al}_2\text{O}_3$ .  
(1 g of Co) (4g of Fe)

## Method 7: co-impregnation method

Catalyst: Co-Fe/Al<sub>2</sub>O<sub>3</sub>



Find Mass: 50g

2.5% : 2.5g metal (Co)

2.5% : 2.5g metal (Fe)

95% : 45g support (Al<sub>2</sub>O<sub>3</sub>)

Ratio → Co:Fe = 4:1

### Calculation:

MW of Co(NO<sub>3</sub>)<sub>2</sub>·6(H<sub>2</sub>O) is 291.03 g/mol

In 291.03 g/mol of Co(NO<sub>3</sub>)<sub>2</sub>·6(H<sub>2</sub>O), has 58.93 g/mol of Co.

In order to get **4g of Co** only, weight of **Co(NO<sub>3</sub>)<sub>2</sub>·6(H<sub>2</sub>O)** that will be used should be **19.7979 g**.

MW of Fe(NO<sub>3</sub>)<sub>3</sub>·9H<sub>2</sub>O is 404 g/mol

In 404 g/mol of Fe(NO<sub>3</sub>)<sub>3</sub>·9H<sub>2</sub>O, has 55.845 g/mol of Fe.

In order to get **1g of Fe** only, weight of **Fe(NO<sub>3</sub>)<sub>3</sub>·9H<sub>2</sub>O** that will be used should be **7.2343 g**.

Thus, **19.7979 g of Co(NO<sub>3</sub>)<sub>2</sub>·6(H<sub>2</sub>O)** + **7.2343 g of Fe(NO<sub>3</sub>)<sub>3</sub>·9H<sub>2</sub>O** + **45 g of Al<sub>2</sub>O<sub>3</sub>** to  
get 50 g of Co-Fe/Al<sub>2</sub>O<sub>3</sub>.  
                        **(4 g of Co)**    **(1g of Fe)**

Figure 27: XRD Pattern for Fe/Al<sub>2</sub>O<sub>3</sub>

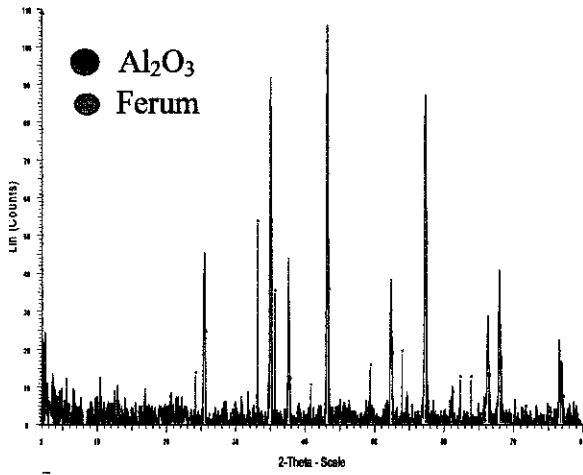


Figure 28: XRD Pattern for Co-

Fe/Al<sub>2</sub>O<sub>3</sub>(sequential)

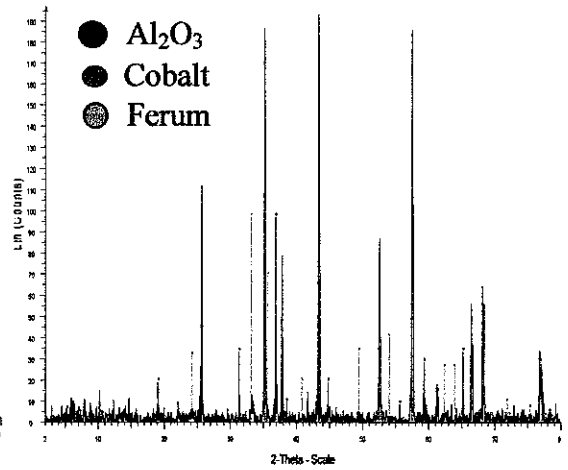


Figure 29: XRD Pattern for Fe-Co/Al<sub>2</sub>O<sub>3</sub> (sequential)

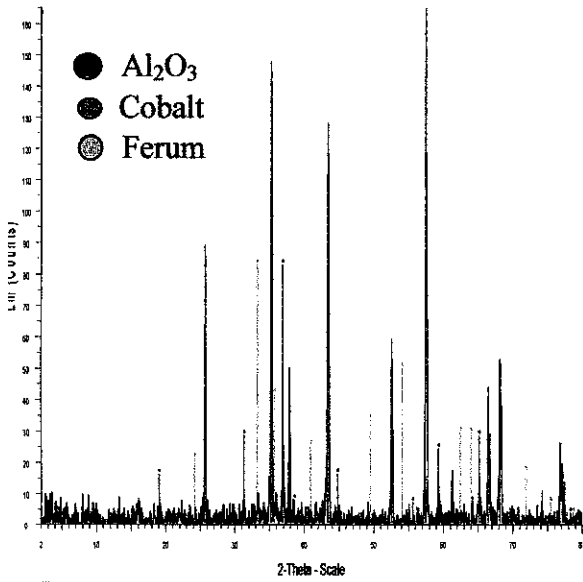


Figure 30: XRD Pattern for Co-Fe/Al<sub>2</sub>O<sub>3</sub> (co-impregnation method)

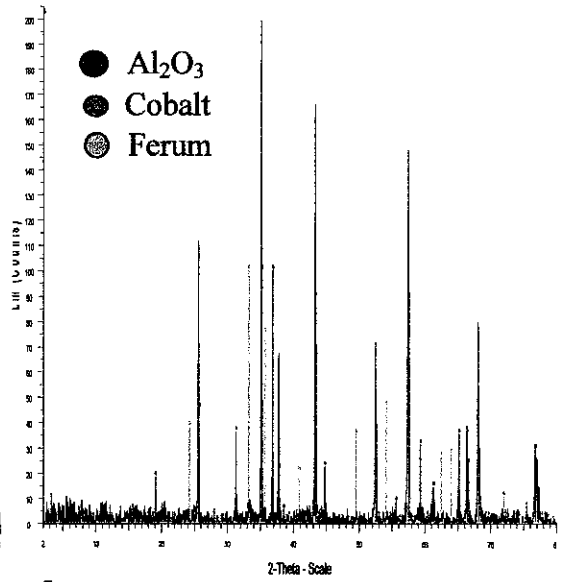


Figure 31: XRD Pattern for Co/Al<sub>2</sub>O<sub>3</sub>

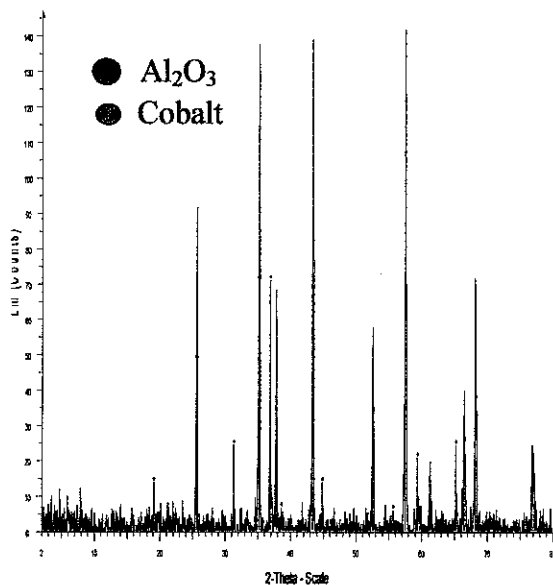


Figure 32: XRD Pattern for Co-Fe/Al<sub>2</sub>O<sub>3</sub>

for Ratio Co:Fe=1:4

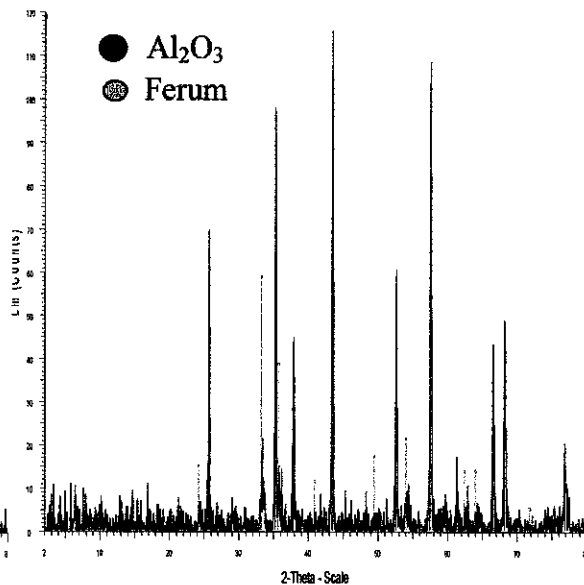


Figure 33: XRD Pattern for Co-Fe/Al<sub>2</sub>O<sub>3</sub> for Ratio Co:Fe=4:1

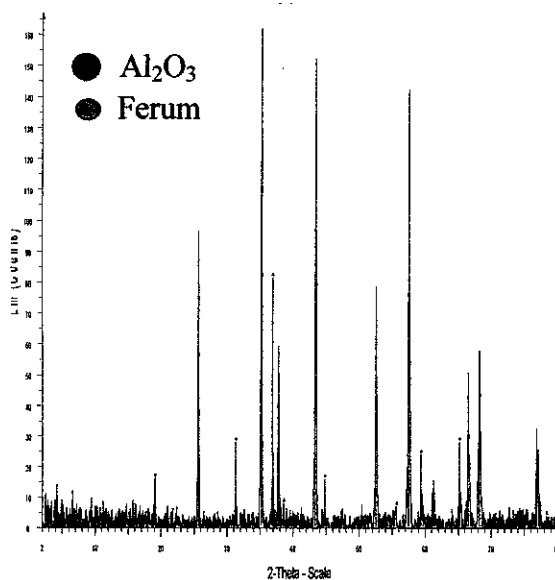


Figure 34: XRD Pattern for  $\alpha$ -Alumina and  $\gamma$ -Alumina

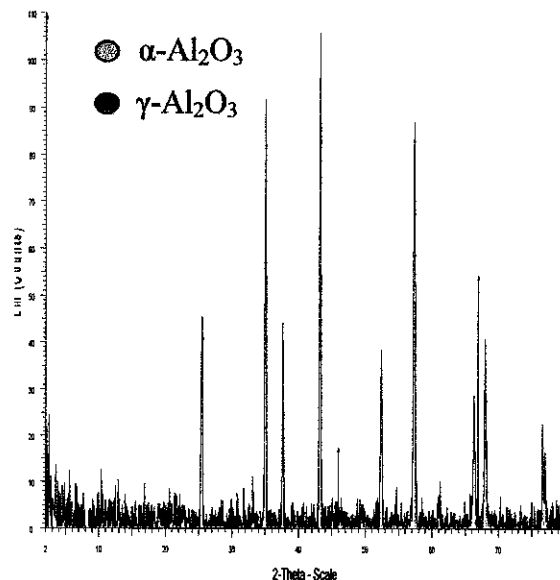
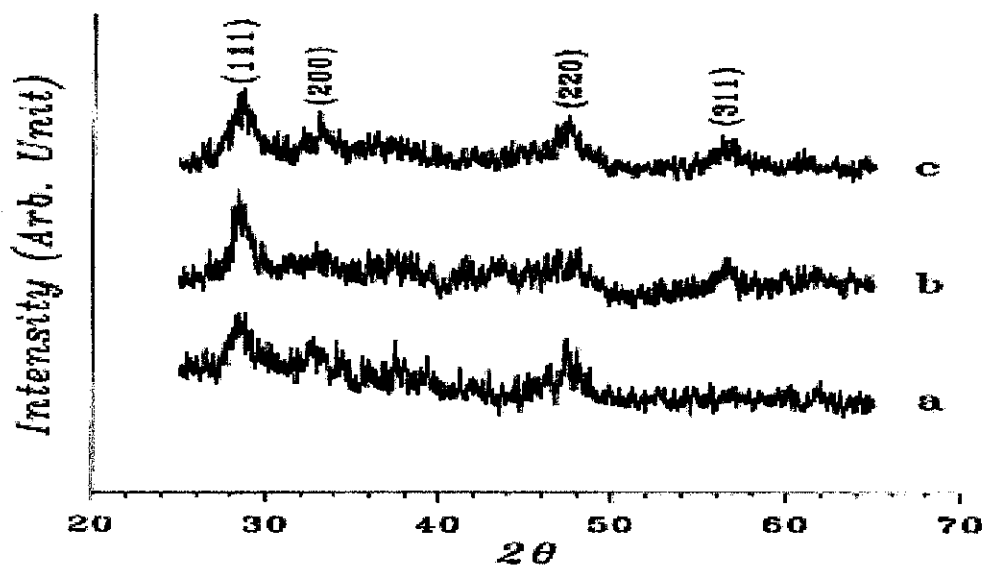


Figure 35: XRD Pattern of supported  $CeO_2$  and YDC. Samples: (a)  $Ce_{10}/\gamma$ -alumina, (b) 5YDC/ $\gamma$ -alumina, (c) 10YDC/ $\gamma$ -alumina



Higher yttria content results in a weaker and broader XRD intensity of copper oxide [13].